

**EFFECTS OF SCROTAL INSULATION ON
SPERMATOZOAL MORPHOLOGY AND CHROMATIN
STABILITY TO ACID DENATURATION IN THE BOVINE**

by

Nicole Acevedo

Submitted to the Faculty of the Virginia Polytechnic Institute and State University in
partial fulfillment of the requirements for the degree of

Master of Science

in

Dairy Science

Richard G. Saacke, Chair

Ludeman A. Eng

William D. Hohenboken

James W. Knight

April 26, 2001
Blacksburg, Virginia

Keywords: sperm chromatin stability, acridine orange, testicular thermal insult

Copyright 2001, Nicole Acevedo

**EFFECTS OF SCROTAL INSULATION ON
SPERMATOZOAL MORPHOLOGY AND CHROMATIN
STABILITY TO ACID DENATURATION IN THE BOVINE**

by
Nicole Acevedo

(ABSTRACT)

The sperm chromatin structure assay (SCSA), as developed by Evenson et al.(1980), utilizes flow cytometry to quantify the susceptibility of sperm chromatin to *in situ* acid denaturation via the metachromatic properties of acridine orange. SCSA is repeatable and has been used to distinguish between fertile and subfertile males in different species; however, it does not permit morphological evaluation of cells. In the present study, the SCSA was modified for the fluorescence/differential interference contrast (DIC) microscope to examine morphology and chromatin stability on the same cell. Semen from six Holstein bulls was collected twice weekly for six weeks. Semen was cryopreserved after collection. A 48-hr scrotal insulation was applied after the first three collections to exert a mild thermal insult to the testes; this induces specific spermatozoal morphological abnormalities to appear in a predictable chronological order, as determined by Vogler et al. (1993). Using DIC optics, sperm head morphology was classified as normal, slightly misshapen, pyriform, severely misshapen, or tailless. Vacuolization in the head region was scored separately as apical, diadem, or random. SCSA and modified-SCSA for fluorescence microscopy were used to assess chromatin instability in the samples. The SCSA parameter of 'cells outside the main population of alpha t' (%COMP_{ot}) and the modified-SCSA parameter of '% cells shifted from green' were positively correlated ($r=0.84$; $P<0.01$). Both variables were positively correlated with the appearance of tailless, pyriform, severely misshapen, and randomly vacuolated

cells ($P < 0.01$), but not with the appearance of diadems or apical vacuoles. Also, the fluorescence microscope detected a significant shift from green in normally shaped cells appearing in morphologically abnormal ejaculates ($P < 0.01$). These results demonstrate that scrotal insulation-induced morphological abnormalities in spermatozoa signify a perturbation in chromatin structure, and that the chromatin perturbation extends into normally shaped cells in the same ejaculate.

ACKNOWLEDGEMENTS

I have to give the greatest thanks to Dr. Saacke for his tremendous wisdom, patience and understanding throughout this process we call “higher learning”. You have been a tremendous advisor and friend, and I feel very fortunate to be the ‘last one’ under your wings. You have encouraged and challenged me every step of the way on this journey, even when I’m the one throwing obstacles in my way. Thanks for everything!

I also have to give the most sincere thanks to Judy Bame for all her help over the past few years. Judy, I really couldn’t have done it without your guidance and good humor !

I couldn’t possibly leave out all my bulls that so generously donated in the name of science. You are all studs in my book.

Special thanks to Larry Kuehn and Dr. Hohenboken for all your statistical advice and help with my data analysis. Larry, I still owe ya a good cup of coffee!

To my committee members Dr. Eng, Dr. Hohenboken, and Dr. Knight--thank you for your participation in this important step in my academic life.

A huge thank you to my fellow graduate students- I can’t imagine having done this without you guys. Special thanks to Sarah for being such a great ‘roommate’ (or would that be flatmate, mate?) and friend. May you never lose the glorious ability to plan your life around your vacations! Thanks to Carrie and Anneke for always lending a helping hand when I needed one, and to Colleen for her amazing kindness and good humor.

Many thanks to Dave for all the great cups of java he brews to keep me alive. Dave, thanks a million for all the little random things and questions you have helped me with over the years. I guess there’s a price for being too smart. . .just kidding!

Many thanks to all my family and friends that keep me sane and strong. I love you all and will carry you all with me wherever I may go. A special thanks to Ray for being the very best friend a person could wish for.

I would like to thank the National Association of Animal Breeders for their financial support of this project and send a special thank you to Don Evenson and the 'South Dakota crew' for sharing your facilities, wisdom, and hospitality with me in gathering my SCSA data.

TABLE OF CONTENTS

(ABSTRACT)	ii
ACKNOWLEDGEMENTS	iv
TABLE OF CONTENTS	vi
LIST OF FIGURES	viii
LIST OF TABLES	x
Chapter I	1
INTRODUCTION	1
Chapter II	3
LITERATURE REVIEW	3
Sperm Chromatin Structure	3
Semen Quality and Fertility	5
Semen Quality and Early Embryo Development	6
Thermoregulation of the Testes	8
Impaired Testicular Thermoregulation and Embryonic Development	11
Detection of Abnormal Chromatin and DNA Damage in Spermatozoa	11
The Sperm Chromatin Structure Assay (SCSA) and Fertility	13
Modification of SCSA for the Conventional Fluorescence Microscope	16
Chapter III	18
DEVELOPMENT OF THE ACRIDINE ORANGE ACEVEDO (AOA) CHROMATIN STRUCTURE ASSAY	18
Chapter IV	25
MATERIALS AND METHODS	25
Objectives	25
Semen Collection	25
Thermal Insult of the Testes and Experimental Design	25
Semen Cryopreservation	26
Sperm Morphology Assessment	27
Sperm Motility Assessment	28
AOA Chromatin Structure Analysis	28
SCSA (Flow Cytometric) Analysis	30
Statistical Analysis	32
Chapter V. RESULTS	34

Chapter VI	59
DISCUSSION	59
REFERENCES.....	63
APPENDICES.....	68
CURRICULUM VITAE	72

LIST OF FIGURES

Figure 1. The effects of 48-h scrotal insulation on overall abnormal sperm head morphology and nuclear vacuolization across bulls (n=6). Data represented as means (\pm SE).....	36
Figure 2. Means (\pm SE) in the percentage of decapitated spermatozoa (A) and diadem defect (B) in relation to the 48-h scrotal insult across all bulls (n=6).....	37
Figure 3. Means (\pm SE) in the percentage of apical vacuoles (A) and random vacuoles (B) in relation to the 48-h scrotal insult across all bulls (n=6).....	38
Figure 4. Means (\pm SE) in the percentage of pyriform (A) and severely abnormal spermatozoa (B) in relation to the 48-h scrotal insult across all bulls (n=6)	39
Figure 5. Response of Bull A to 48-h scrotal insulation based on the appearance of specific abnormal cell types in the ejaculate. Bull A is an overall high responder in terms of an overall increase in morphological aberrations due to the thermal stress. (AV= apical vacuoles; diadem= diadem vacuoles).....	41
Figure 6. Response of Bull B to 48-h scrotal insulation based on the appearance of specific abnormal cell types in the ejaculate. Bull B is also an overall high responder in terms of an overall increase in morphological aberrations due to the thermal stress. (AV= apical vacuoles; diadem= diadem vacuoles).....	42
Figure 7. Response of Bull C to 48-h scrotal insulation based on the appearance of specific abnormal cell types in the ejaculate. Bull C is a moderate responder in terms of an overall increase in morphological aberrations due to the thermal stress. (AV= apical vacuoles; diadem= diadem vacuoles).....	43
Figure 8. Response of Bull D to 48-h scrotal insulation based on the appearance of specific abnormal cell types in the ejaculate. Bull D is a unique moderate responder because of a marked appearance of the diadem defect and apical vacuoles in the absence of misshapen heads. In addition, this degree of response measured in terms of an overall increase in morphological aberrations due to the thermal stress. (AV= apical vacuoles; diadem= diadem vacuoles).....	44
Figure 9. Response of Bull E to 48-h scrotal insulation based on the appearance of specific abnormal cell types in the ejaculate. Bull E is a low responder in terms of an overall increase in morphological aberrations due to the thermal stress. (AV= apical vacuoles; diadem= diadem vacuoles).....	45

Figure 10. Response of Bull F to 48-h scrotal insulation based on the appearance of specific abnormal cell types in the ejaculate. Bull F is the lowest responder in terms of an overall increase in morphological aberrations due to the thermal stress. (AV= apical vacuoles; diadem= diadem vacuoles).....	46
Figure 11. The relationship between the percent of total primary abnormalities and the percent motility across all bulls (n=6) throughout the collection period.	49
Figure 12. The relationship between the changes in chromatin structure represented by %COMP α t (SCSA) and %SHIFT (AOA) and the appearance of specific primary abnormalities induced by the 48-h scrotal insulation in bulls A and B.	51
Figure 13. The relationship between the changes in chromatin structure represented by %COMP α t (SCSA) and %SHIFT (AOA) and the appearance of specific primary abnormalities induced by the 48-h scrotal insulation in bulls C and D.	52
Figure 14. The relationship between the changes in chromatin structure represented by %COMP α t (SCSA) and %SHIFT (AOA) and the appearance of specific primary abnormalities induced by the 48-h scrotal insulation in bulls A and B.	53
Figure 15. Scattergram and histogram representations of SCSA data for Bull A (highest responder) on A) control pre-insult semen sample and B) Day 27 post-insult semen sample.....	55
Figure 16. Scattergram and histogram representations of SCSA data for Bull F (lowest responder) on A) control pre-insult semen sample and B) Day 27 post-insult semen sample.....	56
Figure 17. Digital images representing AOA data for Bull A (highest responder) on A) control pre-insult semen sample and B) Day 27 post-insult semen sample.....	57
Figure 18. Digital images representing AOA data for Bull F (lowest responder) on A) control pre-insult semen sample and B) Day 27 post-insult semen sample.....	58

LIST OF TABLES

Table 1. Analysis of Variance (ANOVA) of Specific Primary Abnormalities Induced by a 48-h Testicular Thermal Insult.....	35
Table 2. ANOVA of Percent Post-Thaw Motility.....	35
Table 3. ANOVA of SCSA and AOA Variables	35
Table 4. Correlation Coefficients (r values): Associations between Specific Primary Abnormalities and Motility	47
Table 5. Correlation Coefficients (r values): Relationship between Chromatin Structure Assay Variables (SCSA and AOA) and Abnormal Morphology and Motility.....	47
Table 6. Correlation Coefficients (r values): Associations Between Chromatin Structure Assay Variables (SCSA and AOA).....	47

Chapter I.

INTRODUCTION

Reproductive efficiency in domestic animals is of major economic concern to breeders. Nearly 90% of the variation in reproductive success of a mating can be accounted for by the initial fertilization rate and by embryonic development through the stage of maternal recognition of pregnancy (Sreenan and Diskin, 1983). Seminal quality impacts both fertilization rate and embryo quality. Seminal deficiencies impacting fertilization rate are predominantly spermatozoal viability and severely distorted sperm morphology that are often masked by inseminate dosage, becoming most important when artificial insemination is employed. On the other hand, the incompetence of fertilizing sperm in sustaining the embryo results in subfertility or sterility at any dosage (under conditions of natural or artificial insemination). Unfortunately, recognition of spermatozoa capable of fertilization but incapable of sustaining the early embryo has not been achieved.

Several studies have demonstrated that impairment of proper testicular thermoregulation results in a reduction of fertility and an increase in early embryonic failure (Young, 1927; Dutt and Simpson, 1957; Bellve, 1972; Setchell et al., 1988). Saacke et al. (1994) showed that insemination of semen from scrotally insulated bulls with a high proportion of nuclear vacuoles on otherwise normal appearing sperm yielded increased proportions of degenerate embryos.

The sperm chromatin structure assay (SCSA) developed by Evenson (1980) has been used to establish a relationship between fertility and the state of chromatin condensation in the sperm nucleus. SCSA has also proved useful in elucidating the effects of heat stress on sperm chromatin structure. However, little has been done to incorporate the SCSA technique into the current repertoire of protocols for selecting bulls and ejaculates in the AI industry. The failure to incorporate the SCSA technique at an industry-wide level can be attributed to a couple of factors. Primarily, it is still unclear whether or not the SCSA evaluation elucidates sperm characteristics that cannot be identified through current evaluation variables of disturbed spermatogenesis, namely,

sperm morphology. Also important is the fact that the flow cytometry instrumentation essential for the SCSA technique established by Evenson et al. (1980) is a costly investment for most academic and industrial laboratories interested in the evaluation of semen.

It is likely that the state of the condensed chromatin in the sperm head is important to early embryonic development in cattle. Since sperm head morphology is associated with early embryonic degeneration, we hypothesize that chromatin perturbations are additive, in information, to morphological abnormalities of the sperm head in judging semen quality. In this study, we applied a 48-h mild scrotal insult to bulls to produce a chronological ejaculation of specific morphological abnormalities over an established collection period (Vogler et al., 1993). This permits the determination of relationships between specific sperm abnormalities and chromatin instability over time as a result of an impairment of testicular thermoregulation.

The overall objectives of this study were: 1) to modify the SCSA technique for the conventional epifluorescence microscope to qualitatively identify chromatin perturbations in the spermatozoa of bulls subjected to a mild insult of their testicular thermoregulatory system, and 2) to relate the spermatozoal chromatin perturbations observed with the occurrence of specific morphological abnormalities induced by the thermoregulatory insult of the testis.

Chapter II.

LITERATURE REVIEW

Sperm Chromatin Structure

Spermatogenesis is the biological transformation of spermatozoa from spermatogonia that requires 61 days for completion in the bull (Johnson et al., 1994). Two major processes, spermatocytogenesis and spermiogenesis, characterize this transformation. Spermatocytogenesis requires approximately 44 days and includes the mitotic and meiotic divisions of spermatogonia to primary and secondary spermatocytes, and then eventually to round spermatids. Spermiogenesis requires an additional 17 days and encompasses the morphological transformation of the round spermatid into the elongated mature spermatozoon (Johnson et al., 1994).

During the process of spermiogenesis, the chromatin structure of the spermatid is dramatically rearranged and the DNA is condensed into a much smaller volume than it occupies in the precursor cells (Ward and Coffey, 1991). Throughout spermiogenesis, transitional proteins gradually replace somatic cell-like histone proteins. Protamines, which are rich in thiol (sulfhydryl) groups ultimately replace the transitional proteins. Two different classes of protamine molecules, protamine 1 and 2, have been differentiated from mammalian sperm, but bull spermatozoa only contain protamine 1 (Balhorn et al., 1991). The replacement process of protamines for histones is believed to be perturbed in the production of abnormal sperm (Kosower et al., 1992). Balhorn (1982) proposed that these protamines bind to the DNA by lying lengthwise along the minor groove of the double-stranded molecule. More recent analyses of DNA-protamine interactions using optically detected magnetic resonance argue that the bull protamine 1 binding site is the major groove of DNA (Prieto et al., 1997). Regardless of specific groove placement, these protamines contain enough positively charged arginine groups to neutralize the negatively charged phosphate groups on the DNA strand. The amino- and carboxy-terminal ends of the bull protamine molecule are folded inward toward the

center of the molecule and are locked into place, each by a single intramolecular disulfide bond (Balhorn et al., 1991). During the final phase of spermiogenesis up to spermiation and even during transport through the rete testis and epididymis, the thiol groups undergo continual oxidation resulting in the many disulfide groups (S-S) that give the chromatin its high degree of compaction and stability in ejaculated sperm. In this process, three intermolecular disulfides cross-link across neighboring protamine molecules to solidify the molecular compaction (Balhorn et al., 1991). This compaction appears important to normal sperm shape and function as well as timeliness of decondensation in association with pronuclear formation (Qiu et al., 1995).

McPherson and Longo (1993) demonstrated the presence of endogenous nicks, or small breaks, in the DNA of elongating rat spermatids. These nicks occur at the time when the chromatin structure is undergoing dramatic transformations. McPherson and Longo (1993) postulate that the DNA topoisomerase II is the endogenous nuclease responsible for creating and ligating nicks during spermiogenesis, and that these nicks may be instrumental in providing relief of torsional stress during DNA condensation. Sakkas et al. (1995) propose that the ligation of the nicks provides the final structural event in the chromatin structure to allow the protamines to associate with and further compact the sperm chromatin; their data suggest that the protamination procedure is completed upon spermatozoal entry into the efferent ducts. Therefore, nicks in the chromatin should not extend into the normally condensed nucleus of ejaculated spermatozoa. Men with a high percentage of endogenous chromatin nicks in their ejaculated spermatozoa (>10% nicks) produced almost double the number of unfertilized oocytes than males with a low occurrence of endogenous nicks (Sakkas et al. 1999). This suggests a necessity for sperm DNA strand integrity in order to carry through successfully the process of fertilization and consequently early embryonic development.

The most integrated model for sperm chromatin packaging depicts an assembly of chromosomes starting as long strands of DNA that are gradually packaged at four levels of organization within the mature spermatozoon (Ward, 1997; Ward and Coffey, 1991). The first level of organization includes the chromosomal anchoring at the nuclear annulus, followed by sperm DNA loop domain organization on the nuclear matrix, protamine decondensation, and finally chromosome organization. The nuclear annulus is

a single structure located at the base of the head and it has been demonstrated in hamster and human sperm that every chromosome has at least one attachment site to the nuclear annulus (Ward and Coffey, 1991). Protamines are complexed with the DNA and permit linear, side-by-side arrays of sperm chromatin along the length of the nucleus (Balhorn, 1982). The linear arrays of protamine packaged chromatin strands are then organized into DNA loop domains that are attached at their bases to a sperm nuclear matrix, the proteinaceous skeletal structure of the nucleus (Ward and Coffey, 1991). In somatic cells, metabolically active genes are specifically associated with the nuclear matrix and effective gene transcription is dependent on a specific association of the genes and the matrix (Stief et al., 1989). As important, Pardoll et al. (1980) described how somatic cell DNA replication occurs at specific sites on the nuclear matrix. In hamster spermatozoa, several genes have a specific spatial relationship with the nuclear matrix, suggesting that sperm DNA loop domains are also organized in a specific, three-dimensional manner on the nuclear matrix (Ward and Coffey, 1991). Mature sperm nuclei do not replicate DNA or transcribe RNA (Stewart et al., 1984) so the need for such a specific organization of sperm DNA loop domains is not clearly understood.

Ward and Zalensky (1996) offer several possibilities for this level of sperm chromatin organization. Sperm DNA loop domain organization may play a role in sperm DNA condensation, or be reminiscent of transcription or replication that occurred during spermatogenesis. McCarthy and Ward (2000) recently presented evidence that the structural integrity of the mouse sperm nuclear matrix may be necessary for the proper unpackaging of sperm DNA for participation in embryogenesis. They determined that even very subtle disturbances to the sperm nuclear structure might have a significant impact on embryo development.

Semen Quality and Fertility

Historically, seminal deficiencies that impact fertilization rate are predominantly spermatozoal viability and more severely distorted sperm morphology which are often masked by inseminate dosage. These deficiencies become most apparent and important when artificial insemination is employed. Salisbury and Van Demark (1961) proposed that the optimum fertility of a female could be increased by increasing the number of

quality sperm delivered, but only up to a threshold number, after which fertility cannot be improved by numbers of sperm in the inseminate. Saacke et al. (1994) described those deficiencies in semen that preclude the availability of sperm for fertilization as ‘compensable traits’ because they can be minimized by increasing inseminate dosage. Compensable traits control the minimal numbers of sperm required for an inseminate to reach maximum fertility (Saacke et al., 2000). Viability traits that can be considered compensable include percent progressively motile sperm and the percent of cells with intact cell or acrosomal membranes (Pace et al., 1981). Factors that impair progressive motility of sperm, such as sperm tail defects or protoplasmic droplets, impede their access to the site of fertilization in the oviduct (Mitchell et al. 1985). Primary morphological abnormalities, or those that affect the sperm head region, also play a significant role in determining the population of spermatozoa that reach the site of fertilization. The percentage of sperm with head abnormalities colonizing the oviduct was lower than in the inseminate, suggesting that a selection against morphologically abnormal cells occurs under sustained transport in the female (Kraznawska, 1974). This finding is corroborated by Saacke et al. (1988, 1998) who demonstrated that only the most subtly misshapen heads appear as accessory sperm on the fertilized ova, regardless of the proportion of abnormal heads in the inseminate. Therefore, impaired motility and severity of head distortion appear to be the foremost factors that prevent spermatozoa from contacting the ovum.

Semen Quality and Early Embryo Development

There is convincing evidence that factors associated with lowered sperm quality may result in reduced embryo quality or in the failure of the embryo to induce maternal recognition of pregnancy (Courot and Colas, 1986; Dejarnette et al., 1992; Orgebin-Crist and Jahad, 1977; Setchell, 1998). This degree of seminal deficiency, characterized by spermatozoal incompetence after fertilization, is defined as ‘uncompensable’ since it cannot be minimized or eliminated by sperm dosage alone (Saacke et al., 2000). Evaluation of accessory sperm serves as an experimental approach to ascertain the quality and quantity of potential fertilizing sperm in an inseminate. Accessory sperm are the sperm trapped in the zona pellucida of the egg/embryo after fertilization, and therefore

represent sperm capable of nearly all the events necessary for fertilization (Evenson, 1999).

Utilizing acceptably fertile Holstein bulls in an artificial insemination center, DeJarnette et al. (1992) found that inseminate of below average quality resulted in a significant reduction in excellent to fair embryos and an increase in degenerate embryos and unfertilized ova relative to that achieved with the insemination of average quality semen. Others have reported a difference among bulls in the quality of their conceptuses recovered for embryo transfer and after observation of embryo survival in the recipients (Miller et al., 1982; Coleman et al., 1987). Bulls differ in the development of their embryos following *in vitro* fertilization (Eyestone and First, 1989) and early cleavage rates are reduced and pronuclear formation delayed in the embryos fertilized by low fertility bulls (Eid et al., 1994). Parrish and Eid (1994) reported that a group of low fertility AI bulls (66 ± 1 % non-return rate) produced embryos having lower cleavage rates to morula or early blastocyst by day 6 of incubation than did a group of high fertility AI bulls (78 ± 1 % non-return rate). Cleaved embryos reaching this stage of development in 6 days were 33% vs 20% for the high and low fertility bulls, respectively, despite the fact that oocyte penetration rates did not differ between the two fertility groups. Also, for the low fertility bulls, pronuclear formation was delayed 1 hour and cleavage to the 2-cell stage was delayed 7 hours indicating the presence of a spermatozoal deficiency adversely affecting embryogenesis at a very early stage.

Few observations are available providing clues toward identification of these incompetent (uncompensable) sperm in semen samples. However, semen containing sperm with misshapen heads and craters has been shown to yield higher frequencies of low quality embryos and lowered fertilization rates than controls where such traits are missing or minimized (Miller et al., 1982; DeJarnette et al., 1992; Saacke et al., 1994). To identify more precisely sperm capable of causing embryonic problems, Saacke et al. (1998) compared the morphological characteristics of accessory sperm in ova/embryos 6 days post artificial insemination with the morphology of sperm inseminated, using the semen of problem bulls. They found that only normally shaped sperm or those deviating slightly from normal in shape appeared as accessory sperm. Thus, the classically recognizable abnormal sperm did not traverse the barriers in the female reproductive tract

or bind to and penetrate the vestments of the ovum. Type of abnormal sperm, i.e. tapered, pyriform, short, etc., was not relevant. Basically, the exclusion of sperm from the fertilization process following insemination in the uterine body was due to the severity of head distortion, not to a specific head shape. Sperm with nuclear vacuoles (craters, diadem, or nuclear pouches, defined by Coulter et al., 1978) were found as accessory sperm at the same frequency as in the inseminate if the vacuoles were found in otherwise normal or only slightly misshapen heads. Thus, potential sperm causing early embryonic death in vivo are most likely normal or very close to normal in shape. Most likely, the competence of a potential fertilization sperm is compromised by defects of the chromatin in the sperm head.

Thermoregulation of the Testes

Proper spermatogenesis in many mammals requires the maintenance of testicular temperature below normal body temperature (Coulter, 1988). Several local mechanisms that play a significant role in testicular thermoregulation include the regulation of blood flow, control of the testis position relative to the body by scrotal musculature, sweating, counter-current heat exchange in the vascular cone, and overall radiation of heat from the scrotal surface (Coulter and Kastelic, 1994). Setchell (1998) suggests that scrotal heating induces scrotal arteriolar dilation through reflex innervation of cutaneous neural receptors. This innervation leads to the removal of sympathetic vasoconstrictor tone and a consequent increase in blood flow. The tunica dartos is a thin sheet of innervated smooth muscle underlying the scrotal skin that responds to changes in ambient temperature. This musculature controls the position of the testis relative to the body wall to enhance a positive abdomino-testicular temperature gradient (Coulter and Kastelic, 1994). The neural reflex of sweating also allows for an exothermic release of heat to precede the evaporation of sweat for cooling. The testicular vascular cone is made up of a complex venous network that surrounds the highly coiled testicular artery. The counter-current heat exchange within the vascular cone functions by allowing a transfer of heat from the warm blood flowing down the testicular artery toward the testis, to the cooler blood returning from the testis through the testicular venous system (Coulter and Kastelic, 1994). Waites and Moule (1961) found that counter-current exchange can only

cool the testis if a temperature gradient exists between the venous and arterial blood, and that the extent of this heat exchange depends solely on the magnitude of the temperature gradient. The vascular cone also plays an important role in the radiation of heat from the scrotum, as the scrotal skin overlying the vascular cone is usually the warmest area on the scrotum (Coulter, 1988).

Kastelic and Coulter (1993) used infrared thermography to assess scrotal surface temperatures (SST) and needle thermistors to measure subcutaneous (SQT) and intratesticular (ITT) temperatures, at the top, middle, and bottom of each testis. The authors found that a positive temperature gradient exists on the scrotal surface and subcutaneous tissue, but that a slightly negative temperature gradient exists within the testicular parenchyma. The positive temperature gradient visualized in the scrotal, and to a lesser degree in the subcutaneous tissue, suggests that the scrotum is cooled in a proximal to distal fashion. The slightly negative temperature gradient observed in the testicular parenchyma suggests that the testicular vasculature helps cool the testes as blood moves up the branching arteries on the caudal-lateral surface toward the dorsal pole of the testis (Coulter and Kastelic, 1994). Kastelic et al. (1996) demonstrated that insulating the scrotal neck of bulls for 48 hours led to an increase in the ITT gradient, but the SST gradient was not significantly different from the pre-insult temperature value. This suggests that scrotal insulation disrupts intratesticular temperature and that the testes is not as adaptable as the scrotum under thermal stress.

In relation to seminal quality, bulls with an inability to thermoregulate the testes have a greater tendency to produce abnormal spermatozoa when exposed to elevated ambient temperatures (Skinner and Louw, 1966; Vogler et al., 1993). Cook et al. (1994) found a decrease in sperm defects associated with a decrease in the average scrotal surface temperature. Kastelic et al. (1996) also found that bulls with insulated scrotal necks had lower percentages of normal spermatozoa and higher percentages of spermatozoa with head defects or droplets than untreated bulls. Vogler et al. (1993) showed that a mild thermal insult to the testis using scrotal sacks raised the testicular temperature approximately 3°C above normal and produced abnormal spermatozoa without affecting sperm output. Specific morphological abnormalities were ejaculated in

a specific chronological order over time, thereby marking an association of specific abnormalities with a period of sperm development or maturation.

Elevated testicular temperatures are shown to alter the structure, motility, or quantity of spermatozoa (Setchell, 1998). As the primary spermatocytes undergo the first meiotic division in the bull, they remain in the pachytene stage of prophase for approximately 10.8 days; the lengthy duration of this stage increases cellular susceptibility to damage and degeneration due to testicular heat stress (Setchell, 1998). Rats exposed to 43 ° C for 15 minutes showed an increase in the number of abnormal pachytene spermatocytes as early as one hour after the insult (Chowdhury and Steinberger, 1970). Increasing the duration of the heat insult reduced the number of pachytene spermatocytes in the rat testis (Wettemann and Desjardins, 1979). Malmgren and Larsson (1989) conducted a scrotal insulation study on boars and showed that after 100 hours of scrotal insult, both pachytene spermatocytes and early spermatids were affected morphologically and quantitatively.

Because of its location in the seminiferous tubule, the Sertoli cell has a profound influence on the developing germ cells as they pass through blood-testis barrier. Germ cells depend almost entirely on Sertoli cells for nourishment and consequent development, therefore marking the Sertoli cell as the most obvious target for thermal perturbation of spermatogenesis (Setchell, 1998). In vitro studies demonstrate that a number of specific genes expressed in Sertoli and germ cells are up- and down-regulated when Sertoli cells are co-cultured with germ cells (Setchell, 1998). This suggests that specific genes in both cell types are important in cell-to-cell communication during spermatogenesis. There is no direct evidence that the Sertoli cells are affected by heat, but subtle changes in the Sertoli cell fluid composition could affect surrounding germ cell chromosome behavior during the meiotic phase (Setchell, 1998).

Heat may also affect the permeability of the plasma membranes of testicular germ cells, as shown by increased leakage of their cellular contents during incubation at elevated temperatures *in vitro* (Lee and Fritz, 1972). As important, there is evidence that DNA synthesis, ascertained through the bioactivity of DNA polymerase beta, is reduced in rat testicular tissue after incubation at 37 ° C (Fujisawa et al., 1997).

Impaired Testicular Thermoregulation and Embryonic Development

Impairment of proper testicular thermoregulation can result not only in a reduction of fertility but in increase of early embryonic failure. The role of the sperm nuclear packing includes both the proper containment of the male genome and the ability of the male genome to carry through early embryonic development. Early *in vivo* studies in guinea pigs and rams demonstrated that a proportion of early embryonic failure was related to male exposure to testicular thermal insult (Young, 1927). Bellve (1972) found that extensive embryonic mortality occurred in mice by day 10.5 of gestation if the male was exposed to an ambient temperature of 34.5 ° C. Setchell et al. (1998) found an increase in the number of degenerating embryos at 2 and 15 days of gestation in female rats mated to males whose testes had been heated to 43 ° C for 30 min. More recently, insemination of semen from scrotally insulated bulls that showed relatively normal viability but high proportions of normal shaped sperm with vacuoles yielded increased proportions of degenerate and low-quality embryos (Saacke et al., 1994). These findings support the assumption that a thermal insult to the testis intensifies the uncompensable component in semen that leads to altered embryo development prior to maternal recognition.

Detection of Abnormal Chromatin and DNA Damage in Spermatozoa

McCosker (1969) was the first researcher to describe a granular appearance of the nuclear chromatin of the spermatozoa of infertile bulls. Gledhill et al. (1971) found that abnormally shaped heads bound up to sixteen times more tritium-labeled actinomycin D than neighboring normally shaped heads. Tritium-labeled actinomycin D binds specifically to DNA and availability of tritium-labeled actinomycin D binding sites on spermatozoa suggests a defect in the condensation of nuclear chromatin. Bedford et al. (1973) found that human spermatozoa are highly heterogeneous compared to the spermatozoa of the rabbit or rhesus monkey, and that many morphologically ‘normal’ spermatozoa show marked differences in the structural integrity of their nuclear

chromatin. Francavilla et al. (1996) demonstrated that staining spermatozoa with alcoholic phosphotungstic acid (PTA) exposed cytochemical defects in the chromatin of both normal and misshapen cells of infertile human males. PTA reacts with histones *in vitro* and readily stains the nuclei of immature spermatids (Courtens and Loir, 1981). The presence of PTA in misshapen spermatozoa may indicate a persistence of histones, or under-protamination, in the cells. Of perhaps greater significance is the prevalence of PTA staining in spermatozoa with normal heads in teratozoospermic ejaculates relative to normozoospermic ejaculates (Francavilla et al., 1996). This finding suggests that a cytochemical chromatin defect was present in a significant number of sperm heads that underwent normal structuring during an altered spermiogenesis.

Several molecular techniques have aided in the elucidation of DNA fragmentation in spermatozoa. Endogenous nicks, or small breaks in the spermatozoal DNA strand, have been analyzed using the *in situ* nick translation assay. This technique works on the basis that DNA polymerase I (Dnase I) can catalyze the movement of endogenous nicks along the double helix, by virtue of its 5'-3' exonucleic activity (Sambrook et al., 1989). More specifically, biotinylated deoxyuridine triphosphate (d-UTP) is added to the Dnase I treated sperm and streptavidin fluorescein-isothiocyanate (FITC) is used to detect the incorporation of biotinylated d-UTP. Therefore, the greater the level of FITC fluorescence in a sample of cells, the greater the degree of endogenous nicks (Sakkas et al., 1995). The percentage of spermatozoa in an ejaculate with endogenous nicks has been negatively correlated with fertility (Bianchi et al., 1993, 1996; Manicardi et al., 1995; Sakkas et al., 1996).

Other molecular techniques include the terminal uridine nick end-labelling (TUNEL) assay, which uses fluorescence labelling to detect DNA fragmentation similar to *in situ* nick translation (Gorczyca et al., 1993) and the Comet assay, which examines DNA strand breaks via single-cell microgel electrophoresis (Aravindan et al., 1997). The sperm chromatin structure assay (SCSA) defines abnormal chromatin structure as the susceptibility of DNA to acid denaturation *in situ* (Evenson et al., 1980). Aravindan et al. (1997) established a significant relationship between the Comet, SCSA and TUNEL assays in human sperm samples. Therefore, the susceptibility of sperm DNA to acid or heat denaturation is correlated to DNA fragmentation. Sailer et al. (1995) postulate that

during spermiogenesis, the endonuclease-derived strand breaks needed for chromatin reorganization are unable to ligate properly and result in residual strand breaks in the spermatozoa. These residual strand breaks in turn are postulated to lead to an altered chromatin structure due to insufficient protamination of the chromatin (Sakkas et al., 1995).

The Sperm Chromatin Structure Assay (SCSA) and Fertility

SCSA is a flow cytometric assay that uses the metachromatic properties of the acridine orange fluorochrome to test the susceptibility of sperm DNA to acid-induced denaturation *in situ* (Evenson et al., 1980). When excited by a blue laser light (488nm), acridine orange (AO) fluoresces green when intercalated into double-stranded DNA (dsDNA), and fluoresces red when bound to single-stranded DNA (ssDNA). Thus, DNA denaturation results in an overall shift from green to red fluorescence (Kapuscinski et al., 1982). The extent of DNA denaturation is quantitated by the computer-calculated ratio of red fluorescence/(red+green) fluorescence expressed as *alpha t* (α) (Darzynkiewicz et al., 1975). The variables measured using α include the mean of *alpha t* ($\bar{x} \alpha$), the standard deviation of *alpha t* ($SD\alpha$), and the percentage of 'cells outside the main population' of α ($\%COMP\alpha$); these values are generated on 5000 cells per sample (Evenson and Jost, 1994). The $\bar{x} \alpha$ indicates shifts and trends in the whole population of cells, whereas the $SD\alpha$ describes the degree of cell-to-cell variation for α in a population (Evenson and Jost, 2000). The $\%COMP\alpha$ indicates the percent of cells with denatured DNA. Although both $SD\alpha$ and $\%COMP\alpha$ measure the level of denaturation within a population, $\%COMP\alpha$ is more descriptive if the entire population shifts from green to red, whereas $SD\alpha$ is more descriptive if a small percentage of cells have shifted to various degrees (Evenson and Jost, 1994). In terms of fertility assessment, $\%COMP\alpha$ is the most important SCSA variable; fertilization attempted by *in vivo* or *in vitro* methods are likely to fail if a population of sperm cells exhibit 30% or more $\%COMP\alpha$ (Evenson, 1999).

The SCSA technique developed by Evenson and Jost (1994) has been used to establish a relationship between fertility and the susceptibility of DNA to denaturation in

bulls (Evenson et al., 1980; Ballachey et al., 1988; Dobrinski et al., 1994; Karabinus et al., 1997), humans (Evenson et al., 1980; Evenson, 1999), boars, (Evenson and Jost, 1994), mice, (Ballachey et al., 1986), and stallions (Sailer et al., 1995; Kenney et al., 1995). Several studies have shown a strong negative correlation between the SCSA variables of $SD\alpha$ and $\%COMP\alpha$ with bull fertility, as measured either by non-return rate of the female (Karabinus et al., 1990), or the competitive index based on heterospermic performance among bulls (Ballachey et al., 1988). Evenson (1999) states that $\%COMP\alpha$ is the most sensitive indicator of male fertility potential because it represents the percentage of cells in a sample that have undergone DNA denaturation. From studies compiled from human and domestic species, $\%COMP\alpha$ values of 0-15%, 16-29% and >30% relate to high, moderate, and very low fertility potential respectively (Evenson and Jost, 2000). The current view assumes that the abnormalities quantified by the $\%COMP\alpha$ and $SD\alpha$ most likely reflect the level of damage that exists to a lesser extent in the whole sperm population, and that this level of damage may be sufficient to cause subfertility in the male (Evenson and Jost, 2000).

SCSA has also proved useful in elucidating the structural changes in the chromatin of spermatozoa due to heat stress. Evenson and Karabinus (1991) investigated the detrimental effects of environmental heat stress on bovine semen quality as measured by SCSA. The objective of the study was to determine if SCSA could determine changes in the seminal quality of bulls collected at Select Sires, Inc. (Plain City, OH) over the summer months more readily than conventional semen quality measurements. According to conventional semen quality variables, one group of bulls studied had previous histories of reduced semen quality over the summer months (responders), while bulls in the other group had no such histories (non-responders). Non-responders showed lower baseline values of $\%COMP\alpha$ than responders. The SCSA detected consistent changes in semen quality at least two days earlier than any other semen quality trait. As important, the most sensitive sperm traits for detecting a reduction in semen quality included both the SCSA values of $SD\alpha$ and $\%COMP\alpha$ and the level of total vacuolated sperm in the ejaculate (Evenson and Karabinus, 1991). Karabinus et al. (1997) demonstrated that the chromatin stability of semen collected after a 48-hour mild scrotal insulation was reduced. There was a significant increase in the SCSA values measured from semen

collected 12 days post-thermal insult, the collection period during which ejaculated sperm were presumed in the testes at the time of scrotal insulation (Vogler et al., 1993). The increase in SCSA values correlate with the increase in morphological aberrations in the spermatozoa due to the heat stress (Karabinus et al., 1997). Interestingly, Karabinus et al. (1997) also found a significant increase in %COMP α t in semen that was presumably in epididymal transit at the time of scrotal insulation; this suggests that chromatin changes began to manifest themselves before the onset of morphological disturbances in the spermatozoa.

Love and Kenney (1999) used a stallion model to study the effects of scrotal heat stress on sperm chromatin, and then compared SCSA values to the protamine and disulfide bond levels in the semen samples. Their results suggest that the level of disulfide bonding, as measured by monobromobimane fluorescent labeling of thiol groups, was inversely correlated with the susceptibility of chromatin to denaturation, as determined by SCSA. The elevated testicular temperatures did not alter the level of disulfide bonding in epididymal sperm at the time of the scrotal insulation, and the chromatin stability of the sperm collected up to 10 days after heat exposure remained unaltered (Love and Kenney, 1999). These results disagree with the findings of Karabinus et al. (1997) in the bull with respect to the stability of sperm in the epididymis at the time of a thermal insult. As important, Love and Kenney (1999) did not find a relative change in protamine or histone content across the collections days. These results differ from those of previous researchers that found changes in the protamine and histone content of ejaculated spermatozoa between infertile and fertile human males (Balhorn et al., 1988; Bach et al., 1990). The intrinsic differences in protamine/histone ratios that exist in human sperm, in that as much as 15% of DNA in human sperm remains packaged as histones, may account for the discrepancy in the data among the stallion subjects. Love and Kenney (1999) postulate that the heat stress to the testes may alter or stop the production of an unknown factor in the primary spermatocyte, which is involved in the formation of protamine configuration or disulfide bonds later in spermiogenesis. The authors conclude that this alteration results in a decrease in the formation of disulfide bonds rather than the breakage of disulfide bonds in the epididymis.

Sperm aging *in vitro* also results in the susceptibility of sperm DNA to denaturation. Estop et al. (1993) demonstrated that mouse sperm aged *in vitro* showed chromatin denaturation within one hour of incubation at room temperature. Karabinus et al. (1990) showed that incubation of bull sperm in cryoprotectant media also increased the susceptibility to DNA denaturation *in situ* within 30 minutes. The effect of the sperm aging on chromatin stability may have the greatest impact on assisted reproductive technologies in humans that require sperm incubation. However, Karabinus et al. (1997) were unable to demonstrate an increase in chromatin susceptibility to denaturation in the *in vitro* incubated versus unincubated sperm collected after scrotal insulation.

Modification of SCSA for the Conventional Fluorescence Microscope

In 1984, Tejada et al. developed the first modification of the SCSA for the conventional fluorescence microscope to eliminate the necessity of flow cytometry for the assessment of human sperm chromatin stability with AO fluorescence. This simplified method, termed acridine orange Tejada (AOT), incorporates the same basic principles as SCSA, but relies on human visual interpretation of the fluorescent characteristics of AO intercalated into the sperm nucleus. The major benefit to a microscopic approach to SCSA is a simultaneous evaluation of sperm chromatin status and morphology. Angelopoulos et al. (1998) found a high concordance between the mean percent of morphologically normal sperm, determined through Shorr dye staining, and the percent green sperm determined through AO fluorescence (AOT). Dobrinski et al. (1994) found a correlation between red fluorescing cells and the percentage of pyriform heads and vacuoles. However, they also found that high numbers of abnormally condensed nuclei can be found in the absence of other defects (Dobrinski et al., 1994). Several laboratories have used the AOT technique to assess male fertility potential (Ibrahim and Pedersen, 1988; Roux and Dadoune, 1989; Claasens et al., 1992). They have found significant correlations between red fluorescence and abnormal sperm morphology, but not between red fluorescence and motility (Tejada et al., 1984; Ibrahim and Pedersen, 1988). This suggests a potential infertility factor in spermatozoa that is removed from sperm viability alone.

There have been problems reported with the interpretation of AO fluorescence on sperm cells using AOT. Rapidly fading fluorescence and indistinct color are most commonly associated with this technique (Duran et al, 1998; Claasens et al., 1992). Others have modified the technique to enhance the stability of the stain across a variety of species (Dobrinski et al., 1994; Beletti and Mello, 1996). Kosower et al. (1992) resolved that the acridine orange fluorescence of sperm nuclei is determined by the thiol-disulfide status of DNA-associated protamines. Their results indicate that nuclei fluoresce green when spermatozoa are treated with acetic alcohol while their nuclear protamines are rich in disulfide bonds and they fluoresce red when treated with acetic alcohol while their protamines are poor in disulfide bonds (Kosower et al., 1992). This suggests that the structure of chromatin is important for controlling the interaction of AO with DNA. This finding strengthens the SCSA argument that varying degrees of susceptibility to acid denaturing conditions are indicative of abnormal chromatin structure (Evenson et al., 1985). Perhaps the use of thiol-protectant chemicals such as dithiothreitol or 2-mercaptoethanol may help stabilize the chromatin after acid treatment and minimize the present constraints associated with the AOT technique, i.e. rapid quenching and/or shifts in fluorescence color over time. This was the concept we followed in the current work to modify the AOT procedure in order to evaluate effectively and repeatably the chromatin stability of spermatozoa from bulls subjected to a thermal testicular insult.

Chapter III.

DEVELOPMENT OF THE ACRIDINE ORANGE ACEVEDO (AOA) CHROMATIN STRUCTURE ASSAY

The chromatin evaluation procedure developed by Tejada et al. (1984) for the fluorescence microscope (AOT technique) requires modification for bull spermatozoa. Essentially, we have combined the methods of Evenson et al. (1980), Tejada et al. (1984) and Kosower et al (1992), while including essential modifications of our own. The sperm chromatin structure assay (SCSA), developed by Evenson et al. (1980), is a flow cytometric analysis based on the properties of the fluorochrome acridine orange (AO) which fluoresces green when bound to native deoxyribonucleic acid (DNA) and red when bound to denatured DNA (single-stranded). SCSA measures the susceptibility of sperm nuclear DNA to acid-induced denaturation *in situ* by quantifying the metachromatic shift of AO from green to red.

Tejada et al. (1984) introduced a simplified microscopic method of the SCSA to evaluate human spermatozoa that does not require flow cytometric equipment. The Tejada method employs the general SCSA principal of denaturing the cells with a single *in situ* acid treatment and then staining the cells with AO before analysis under a conventional fluorescence microscope. Problems associated with this simplified method include indistinct fluorescence color (Claasens et al., 1992), rapidly fading fluorescence (Duran et al., 1998) and heterogeneous slide staining conditions (Evenson et al., 1980). Kosower et al. (1992) found that the thiol-disulfide status of protamines determines the acridine orange fluorescence of sperm nuclei, and that a small concentration of dithiothreitol (DTT) acts to reduce disulfides and maintain thiols in the experimental sample viewed under conventional fluorescence microscopy. Kvist (1982) elucidated that the increased availability of free thiols induced by DTT may activate the decondensation of sperm nuclear chromatin and allow staining agents access to nuclear components usually masked by condensed chromatin. In our hands, the development of a technique for effectively and repeatably evaluating the chromatin stability of bull spermatozoa under epifluorescence microscopy required the addition of thiol-protectant

agents such as dithiothreitol or 2-mercaptoethanol to help stabilize the thiol-disulfide ratio within the chromatin after acid treatment. This may minimize the present constraints associated with the apparent reoxidation of thiols in the AOT technique.

Cryopreserved semen from a previous testicular insulation study (Degelos, dissertation 1995) was used to establish a set of controls for developing the AO staining technique. Semen was used from pre- and post- scrotal insult days of collection (specifically Day -4 and Day 19 of collection) and spermatozoa were evaluated for quantity and type of primary abnormalities. To maintain consistency, samples were taken from one bull only, and the pre-insult semen (Day 4) contained less than 10 % cells with primary abnormalities, while the post-insult semen (Day 19) contained cells with greater than 50 % primary abnormalities.

The following describes the preliminary procedure used to prepare the sperm cells for AO staining. Briefly, three 0.5 ml straws of frozen semen (either pre-insult or post-insult) were thawed in a 37°C water bath for 30 sec and the contents of the straws were pooled into a graduated centrifuge vial. The volume of the semen was doubled to 3 ml with 2.9% sodium citrate dihydrate buffer and 9mM EDTA solution (pH of buffer solution adjusted to 6.8 with citric acid monohydrate). The semen was extended in 2.9% sodium citrate buffer solution because that is the same buffer solution used in preparing the semen for cryopreservation. EDTA is a chelator that inhibits Ca⁺⁺ or Fe⁺⁺ catalysis; these metal ions can form metal complexes with a thiol and lead to oxidation of the thiol. The concentration of EDTA added is consistent with the concentration in Tyrode's buffer solution (Tejada, 1984). The semen was then washed three times by centrifugation at 755 G (2500 RPM) for 10 min per wash. The final washed sample was resuspended in sodium citrate buffer solution to its original volume of 1.5 ml. The washed semen was then smeared onto Superfrost Plus® microscope slides (Fisher Scientific, Pittsburgh, PA) and allowed to air dry for 10 min (these slides retain cells electrostatically as they are washed and stained).

The air-dried slides were treated with a solution of dithiothreitol (DTT; Sigma Chemical Co., St. Louis, MO) for 30 min. At a pH of 7, DTT acts as a protective agent for thiol groups, and is oxidized to the cyclic disulfide, thereby ensuring the reduction of other disulfides in solution (Sigma® product information). After several modifications of

the Kosower et al. (1992) DTT treatment, we determined that a 0.1 mM solution of DTT (in 2.9% sodium citrate buffer with 9 mM EDTA, pH 6.7) allowed for the greatest degree of color variation after AO staining without compromising morphological integrity. The DTT treated slides were gently washed with buffer solution to remove excess DTT and allowed to air-dry at room temperature with a cool fan for 20 min. Air-drying was implemented to ensure that cells were fixed on the slides between treatments. The treated slides were then immersed in a Carnoy's acid bath (3 parts methanol: 1 part glacial acetic acid; adjusted to pH 1 with 4 N HCL) for 2 h (Kosower et al., 1992). Treatment with Carnoy's served a dual purpose: as both an acid denaturant and a cell fixative. After the acid treatment, the slides were allowed to air dry for 10 minutes. Smears were then stained for 5 min in the dark (at 5°C) with an AO solution (1% special high purity AO, Polysciences Inc., Warrington, PA; 0.1 M citric acid, 0.3 M Na₂HPO₄·7H₂O) as established by Tejada et al (1984). After staining, slides were washed with sodium citrate buffer solution, sealed with Vaseline®-edged coverslips, and maintained in the dark cold environment before evaluation.

Semen evaluation was carried out within 10 min of staining using the epifluorescence microscope equipped with differential interference contrast (DIC) optics (Nikon E600®). A field of sperm was mapped out within the field of view by morphology and the DIC illumination was replaced with epifluorescence illumination, via shutter. The microscope was equipped with a 450-490-nm excitation filter and a 520-nm barrier filter. For each specimen, AO staining and morphology were assessed simultaneously in at least 100 spermatozoa in 10 or more individual fields. The observation time of each individual field did not exceed 40 sec, as established by Angelopoulos et al (1997). The fluorescent characteristics were noted as green (double-stranded, acid resistant DNA), red-orange (single-stranded, denatured DNA), half green-half red (partially denatured DNA), pink or yellow (partially denatured DNA), and then recorded by location in the field of view. This permitted evaluation of data for each specimen by the relationship of chromatin stability to sperm morphology.

Preliminary results showed that our AO staining technique could distinguish between thermally insulted and non-thermally insulted semen samples. Control samples, in which the morphology appeared quite normal, fluoresced a uniform green color under

UV light. Thermally insulated samples showed a variation in abnormal cell types and also showed a variation in fluorescence staining patterns. Our observations indicated that a critical period exists for evaluating the proper fluorescence emission, and that this period should not exceed 10 min post-staining with AO. The samples tended to shift toward an overall green fluorescence within 10 min of the initial viewing, indicating a potential reoxidation of the thiol groups.

Several trials and observations led us to believe that the ambient temperature and the concentration of the reducing agents (such as EDTA and DTT) exert the most influence on the fluorescent stainability of the stained sample. DTT is most stable at a pH of 6.5 at 20°C, however at a pH of 8, DTT can induce complete reduction of disulfides in minutes (Sigma®, product information). Throughout the trials, a great inconsistency occurred between samples using the 0.1 mM concentration of DTT. At times, this concentration would allow for a good degree of color variation to occur and to be maintained in the thermally insulated semen sample after AO staining. However, at other times, the fluorescence faded quite rapidly or the samples would shift to green fluorescence from red, orange, or yellow within 10 min of staining. A rapid increase in the temperature of the stained slide (from 5°C in the cold room to 25°C in the microscope room) resulted in a rapid shift to complete green fluorescence in a perturbed sample. Thus, the slides should be kept in a 5°C insulated cooler after staining until viewing. An important caveat to note is that the slides do not stain uniformly. First of all, the edges of the slides that are covered with Vaseline as well as air bubbles must be avoided for quantification because they reflect skewed spectral properties. Also, since the slides are smeared according to the Shaffer and Almquist method (1948), the majority of the cells are distributed along one half of the slide. The more cells in a field of view, the greater the intensity and maintenance of the fluorescence. Therefore, before a slide was evaluated, it was first scanned over quickly to assess uniformity of staining. Areas that fluoresced entirely green or red were avoided since the fluorescence was most likely artifactual.

We determined that the most objective form of viewing and evaluating the specimens required digital imaging that could be readily adapted to the microscope. This would allow for a more objective and accurate assessment of both morphology and

fluorescence emission under a time constraint. As important, we determined the need for a more stable thiol protectant than DTT to ensure consistency among sample slides. 2-Mercaptoethanol (2-ME; Sigma Chemical Co., St. Louis, MO) proved to offer greater consistency and thus the technique was refined using 2-ME as a thiol protectant.

For the refined technique using 2-ME, three 0.5 ml straws of frozen semen (either pre-insult or post-insult) were thawed in 37°C water bath for 30 sec and the contents of the straws were pooled into a graduated centrifuge vial. The volume of the semen was doubled to 3 ml with 2.9% sodium citrate buffer and 9 mM EDTA solution (pH of buffer solution adjusted to 6.8 with citric acid monohydrate). The semen was then washed three times by centrifugation at 1475 G (3500 RPM) for 10 min per wash. During each wash, the pellet of cells was resuspended to 3 ml with buffer solution and vortexed to ensure proper pellet disruption. The final washed sample was resuspended in sodium citrate buffer solution to its original volume of 1.5 ml and vortexed. The washed sperm were then smeared onto Superfrost Plus® (Fisher Scientific, Pittsburgh, PA) microscope slides according to the Shaffer and Almquist method (1948) and allowed to air dry under a cool fan for 10 min. Air-drying was implemented to ensure that cells were fixed on the slides between treatments.

2-ME is a reagent that can maintain thiol groups in their reduced state if used at a concentration of 10 mM or greater (Sigma® product information). 2-ME is most stable at pH 6-7 with 0.05 mM EDTA; it is also quite stable at room temperature and it is miscible in alcohol. Due to its properties, 2-ME was prepared at a concentration of 56mM in 2.9% sodium citrate buffer and 9mM EDTA solution (pH 6.7), and brought to a final concentration of 7 mM in Carnoy's acid treatment (pH 1.2). The rationale for this step was to stabilize the 2-ME in a buffer solution with EDTA and then to place it in the acid bath at a concentration that would protect the thiols as they formed due to acid denaturation. 2-ME was also prepared at 7mM concentration in the buffer solution and placed in the 5°C cold room for rinsing the slides after AO staining; the addition of 2-ME to the rinsing solution should ensure that the thiols will be further protected from staining until viewing.

The air-dried slides were then immersed in a Carnoy's acid bath (see Appendix B for composition) for 2 h at ambient temperature (23° C). After the acid treatment, the

slides were immediately drained and placed on a staining rack in the cold room. Smears were then stained for 5 min in the dark (at 5°C) with an AO solution (Appendix B) as established by Tejada et al (1984). After staining, slides were washed gently with buffer solution containing 7 mM 2-ME, sealed with Vaseline®-edged coverslips, and maintained in a 5°C insulated cooler after staining until viewing.

Semen evaluation was carried out within 10 min of staining using the epifluorescence microscope powered by a super high-pressure mercury lamp (Nikon Eclipse E600®, Nikon Inc., Melville, NY). The microscope was equipped with a 450-490-nm excitation filter and a 520-nm barrier filter. The Kodak Digital Microscopy Imaging® system (Eastman Kodak Co., New Haven CT) was used to photograph the treated slides. The Kodak® digital camera was mounted onto the Nikon E600® epifluorescence/DIC microscope. The camera was connected to a computer program (MDS 120®, Eastman Kodak Co., New Haven CT) that processes and downloads the digital image through a parent program (Adobe Photoshop®, Adobe Systems, Inc., San Jose, CA) to store the image for future analysis. This process allowed us to photograph a series of fields per slide in a minimal amount of time and objectively analyze the stored images at a later date. Samples were photographed at 400x under epifluorescence microscopy only and viewing of each individual field did not exceed 40 sec, as established by Angelopoulos et al (1997). The fluorescent characteristics were noted as green (double-stranded, acid resistant DNA), red-orange (single-stranded, denatured DNA), half green-half red (partially denatured DNA), pink or yellow (partially denatured DNA).

The revised AO technique is an efficient and stable method of detecting the DNA condensation patterns in bovine spermatozoa. The samples maintained a steady fluorescence emission throughout the image-processing period, therefore a reduction in fluorescence quenching or thiol reoxidation was in effect. 2-ME is a more stable thiol protectant than DTT, and it maintained its integrity and function while in acid. The 2-ME additions prolonged the amount of time necessary to view and photograph the slides to capture the most accurate depiction of DNA denaturation through a fluorescence microscope. The integrity of the AO stain was also aided by maintaining the stained slides in a cold dark environment from staining to viewing. Before a slide was evaluated,

it was first scanned quickly to assess uniformity and intensity of staining to avoid quantification of cells in areas of the slide that reflect skewed spectral properties under fluorescence (such as air bubbles or the edges of the slide). This modified technique for the evaluation of sperm chromatin integrity under fluorescence microscopy will be referred to as the acridine orange Acevedo (AOA) chromatin structure assay.

Chapter IV.

MATERIALS AND METHODS

Objectives

- 1) to modify the SCSA technique for the conventional epifluorescence microscope to qualitatively identify chromatin perturbations in the spermatozoa of bulls subjected to a mild insult of their testicular thermoregulatory system.
- 2) to relate the spermatozoal chromatin perturbations observed with the occurrence of specific morphological abnormalities induced by the thermoregulatory insult of the testis.

Semen Collection

Six Holstein bulls were selected on their ability to produce neat semen having greater than 70 % morphologically normal sperm with 70 % or greater estimated progressive motility. Five bulls ranged in age from 13-15 months and one bull was 24 months of age during the trial period. Semen was collected via artificial vagina. The collection of each ejaculate was preceded by a period of sexual preparation consisting of two false mounts separated by two minutes of active restraint. Bulls were housed at the Bull Research Barn, Virginia Polytechnic Institute and State University, Dairy Cattle Center, Blacksburg, Virginia.

Thermal Insult of the Testes and Experimental Design

Semen was collected at a frequency of two ejaculates in succession every Monday and Thursday beginning two weeks prior to data collection to stabilize semen characteristics and epididymal sperm reserves. Data collection began 8 days prior to a 48-h insulation of the scrotum and continued until Day 34 after the scrotal insulation. The purpose of the thermal insult to the testes was to mimic a mild, naturally occurring

environmental interference with testicular thermoregulation, as described previously by Vogler et al. (1993). Thermal insult of the testes was induced by enclosing the entire scrotum, including the neck, with a sack constructed of insulating material that was fastened in place with Velcro® strips and medical tape (Vogler et al., 1993). The insulation was secured tightly enough to remain in place but not to restrict blood circulation during the insult period. After two hours, allowing for thermal response of the scrotum to the elevated temperature, the sacks were readjusted to assure complete coverage of the scrotum and the scrotal neck. Bulls were monitored every 2 h for the first 12 h of insulation and every 4 h for the final 36 h. Monitoring ensured proper scrotal sack placement and proper bedding and water conditions for the animals during the insult. The thermal insult was maintained for a period of 48 h. Three bulls were placed on the experiment between October and November 1999, and the remaining three bulls were placed on the experiment between March and April 2000.

The pre-insult collection period consisted of Day -8, Day -5, and Day -1, where Day 0 was the day of scrotal sack installation and Day 2 the day of removal. The post-insult collection period encompassed the remaining days through Day 34 post-insult. Semen collected on Day 2 through Day 9 post-insult corresponds to ejaculated sperm that were present in the epididymis and rete testis during the time of scrotal insulation, and spermatozoa collected between Day 13 and Day 34 post-insult represent sperm that were in spermatogenesis at the time of the heat insult (Vogler et al., 1993). Thus, the scrotal insult provided for variation in seminal quality within bulls as well as across bulls based upon their susceptibility to heat.

Semen Cryopreservation

On each collection day, the volume of each ejaculate was measured by weight in graduated collection vials. The two ejaculates from each bull were pooled (2 ml of semen from each collection) and pre-diluted 1:1 with the non-glycerolated fraction of egg yolk-citrate extender (see Appendix A for extender composition). Sperm concentration was determined using a spectrophotometer calibrated for bovine sperm (Spectronic® 20 D, Milton Roy Co., Rochester NY) using a 100 µl aliquot of neat pooled ejaculate for

each bull. Pre-diluted ejaculates were prepared in the conventional manner for cryopreservation at a final concentration of 50×10^6 sperm/ml using egg yolk-citrate containing 7% glycerol v/v (Robbins et al., 1976). Only the ejaculates collected on Day – 8, Day -5, and Day -1 pre-insult and on Day 2, Day 9, Day 13, Day 16, Day 20, Day 27, and Day 34 post-insult were prepared for cryopreservation. Semen collected on these days adequately depict the sperm morphological changes associated with a perturbed spermatogenesis that occur between pre- and post-insult periods (Vogler et al., 1993). Aliquots of pooled raw ejaculates from all other days of collection were placed in Karnovsky's fixative (100 μ l neat semen in 1 ml Karnovsky's fixative) for morphological evaluation (Karnovsky, 1965).

Sperm Morphology Assessment

All semen samples were coded prior to morphological analyses to preclude any bias. Semen samples that were fixed in Karnovsky's were prepared as wet smears. From the semen samples that were frozen, two straws from each bull/collection day were thawed in a 37° C water bath for 30 sec, and then the contents were pooled in a 1.5-ml microcentrifugation tube (polypropylene disposable vials, Fischer Scientific, Pittsburgh, PA). Wet smears were prepared for analysis by placing a drop of thawed semen from a capillary tube on a slide and immobilizing the sperm cells with a drop of 40 mM sodium fluoride, and then gently covering the drop with a coverslip (Mitchell et al., 1978). Morphology was evaluated on 200 cells using differential interference contrast (DIC) microscopy at 1000x magnification under oil. Cell abnormalities were classified according to Barth and Oko (1989).

Defects involving the sperm head, classified as primary abnormalities, are most indicative of a stress on testicular thermoregulation and they appear in a specific chronological order following scrotal insulation (Vogler et al., 1993). The specific primary abnormalities that characterize a disturbance in spermatogenesis due to scrotal insulation include decapitated spermatozoa, vacuolated sperm heads, pyriform-shaped heads, and severely misshapen heads (Vogler et al., 1993). For purposes of quantification, the total percent of abnormal cells included decapitated, pyriform, and

severely misshapen heads; all other cells were categorized as normal or slightly misshapen. Nuclear vacuolization was quantified separately out of the same 200-cell count, so as not to preempt head shape abnormalities; vacuolization was categorized as apical vacuoles, diadem defects, and random vacuoles.

Sperm Motility Assessment

All semen samples were coded prior to motility analyses to preclude any bias. Motility estimates were performed only on the semen samples that were frozen and used for fluorescence analysis. Two straws from each bull/collection day were thawed in a 37° C water bath for 30 sec, and then the contents were pooled in a 1.5-ml microcentrifugation tube (polypropylene disposable vials, Fischer Scientific, Pittsburgh, PA). Wet smears were prepared by placing a drop of thawed semen on a warmed slide and then covered with a warmed coverslip. Motility was assessed at 250x magnification using a phase-contrast microscope equipped with a 39°C-heated stage. Motility was estimated to the nearest 10%.

AOA Chromatin Structure Analysis

All semen samples were coded prior to preparation to preclude any bias. Coded replicates were performed on each semen sample but on separate days of analysis. For each bull, semen from days -8, -5, and -1 were combined to represent a single pre-insult control sample. Semen from days 2 and 9 individually represent sperm present in the epididymis during the insult. Semen from days 13, 16, 20, 27 and 34 individually represent sperm undergoing spermatogenesis at the time of the heat insult. Therefore, sixteen samples (including two replicates per day of collection) per bull represent the total semen collection period assessed for chromatin structure stability. One bull (Bull A) is represented by seven rather than eight samples because of a cryopreservation error with his semen collected on day 9 post-insult.

Three straws of frozen semen from each sample studied were thawed in 37°C water bath for 30 sec and the contents of the straws were pooled into a graduated centrifuge vial. The volume of the semen was doubled to 3 ml with 2.9% sodium citrate dihydrate buffer and 9mM EDTA solution (see Appendix A for buffer composition). The semen was then washed three times by centrifugation at 1475 G (3500 RPM) for 10 min per wash. During each wash, the pellet of cells was resuspended to 3 ml with buffer solution and vortexed to ensure proper pellet disruption. The final washed sample was resuspended in sodium citrate buffer solution to its original volume of 1.5 ml and vortexed. The washed sperm were then smeared onto Superfrost Plus® (Fischer Scientific, Pittsburgh, PA) microscope slides according to the technique of Shaffer and Almquist (1948) and allowed to air dry for 10 min. Air-drying with a cool fan was implemented to ensure that cells were fixed on the slides between treatments.

2-Mercaptoethanol (2-ME) was prepared at a concentration of 56 mM in 2.9% sodium citrate buffer solution (Appendix A), and brought to a final concentration of 7mM in Carnoy's acid treatment (pH 1.2). 2-ME was also prepared at 7mM concentration in the buffer solution and placed in the 5°C cold room for rinsing the slides after AO staining.

The air-dried slides were then immersed in a Carnoy's acid bath (see Appendix A for composition) for 2 hours at ambient temperature (23° C). After the acid treatment, the slides were immediately drained and placed on a staining rack in the cold room. Smears were then stained for 5 min in the dark (at 5°C) with an AO solution (see Appendix B for preparation) as established by Tejada et al (1984). After staining, slides were washed gently with buffer solution containing 7mM 2-ME, sealed with Vaseline®-edged coverslips, and maintained in a 5°C insulated cooler until viewing.

Semen evaluation was carried out within 10 min of staining using the epifluorescence microscope powered by a super high-pressure mercury lamp (Nikon Eclipse E600®, Nikon Inc., Melville, NY). The microscope was equipped with a 450-490-nm excitation filter and a 520-nm barrier filter. The Kodak Digital Microscopy Imaging® system (Eastman Kodak Co., New Haven, CT) was used to photograph the treated slides. The Kodak® digital camera was mounted onto the Nikon E600® epifluorescence/DIC microscope. The camera was connected to a computer program

(MDS 120®, Eastman Kodak Co., New Haven, CT) that processes and downloads the digital image through a parent program (Adobe Photoshop®, Adobe Systems, Inc., San Jose, CA) to store the image for future analysis. This process allowed us to photograph a series of fields per slide in a minimal amount of time and objectively analyze the stored images at a later date. Samples were photographed under epifluorescence microscopy at 400x and viewing of each individual field did not exceed 40 sec, as established by Angelopoulos et al (1997).

For each replicate, AO staining and morphology were assessed simultaneously in 200 spermatozoa in 10 or more individual fields. The fluorescent characteristics of each cell were noted as either green (double-stranded, acid resistant DNA), red-orange (single-stranded, denatured DNA), half green-half red (partially denatured DNA), pink or yellow (partially denatured DNA). The morphological characteristics were categorized more generally since the fluorescence imaging did not always permit the evaluation of vacuoles or tails on the sperm. Therefore, sperm heads were classified as either normal or distorted in overall shape. This general classification of normal heads did not allow for the distinction between decapitated and intact sperm heads, but it did allow for a basic distinction between abnormal shaped and relatively normal shaped cells. For each replicate, a percentage was calculated for the total number cells that shifted away from green fluorescence (%SHIFT), regardless of morphology. %SHIFT represents the total percentage of cells exhibiting some degree of susceptibility to *in situ* acid denaturation of their sperm chromatin. The percentage of cells (from the total sperm count) with quantifiably normal morphology that shifted from green fluorescence were labeled as %SHIFT NORMAL.

SCSA (Flow Cytometric) Analysis

The sperm chromatin structure assay (SCSA) was performed as described by Evenson and Jost (2000). Two successive replicates were performed per bull sample. Briefly, two separate straws of semen from each sample studied were thawed in a 37° C water bath for 30 sec and the semen was pooled into a test tube then diluted to 1-2 x 10⁶ sperm/ml with TNE buffer (see Appendix C for buffer composition). The diluted semen, buffer, and staining solution were kept on crushed liquid ice throughout the preparation process. Two hundred µl of the diluted sperm suspension were treated with a 400 µl

acid-detergent solution for 30 sec (Appendix C) to permeabilize the cell membrane and allow the AO fluorochrome to enter the sperm nucleus. The low pH solution partially denatures the DNA in the sperm with abnormal chromatin structure; the DNA in sperm with normal chromatin structure is resistant to this level of physical stress (Evenson and Jost, 2000). After the 30 sec acid treatment, the cells are stained with 1.20 ml of AO staining solution (Appendix C). The prepared, stained sample was placed on the flow cytometer sample chamber in a 30-ml beaker containing ice water slurry to maintain temperature equilibrium. Three minutes after the staining procedure began, red and green fluorescence measurements were collected on 5000 cells per sample using an Ortho Diagnostic Cytofluorograf II (Becton Dickinson, Westwood, MA) with a closed quartz flow cell and a 100 mW argon ion laser operated at 35 mW power. The flow cytometer was interfaced to a Cicero computer unit with PC-based Cyclops software (Cytomation, Fort Collins, CO). The three minutes before data collection allowed for AO equilibration in the sample and hydrodynamic stabilization of the sample within the fluid. (Evenson and Jost, 2000). The rate of sperm cell measurement should not exceed 300 cells/sec to allow for the proper quantification of fluorescence emission per cell (Evenson and Jost, 2000). Replicates are performed in succession from the same thawed aliquot of semen. All the semen samples in the experiment are run on the flow cytometer and then analyzed as a group (Evenson and Jost, 2000).

The extent of DNA denaturation is quantitated by the computer-calculated ratio of red fluorescence/(red+green) fluorescence expressed as alpha t (αt) (Darzynkiewicz et al., 1975). The SCSA results for each sperm sample analyzed are expressed as the mean of alpha t ($\bar{x} \alpha t$), the standard deviation of alpha t ($SD \alpha t$), and the percentage of 'cells outside the main population' of αt ($\%COMP \alpha t$). The $\bar{x} \alpha t$ describes the average αt value for the sperm analyzed in the semen sample. The $SD \alpha t$ reflects the sperm-to-sperm variation for αt within a sample, whereas the $\%COMP \alpha t$ indicates the percentage of sperm with an increased susceptibility to DNA denaturation and consequently abnormal chromatin structure (Evenson and Jost, 2000).

The data are gathered into a data set and statistically analyzed by the Cicero computer unit with PC-based Cyclops software (Cytomation, Fort Collins, CO). The data set for each sample is then formulated into cytograms and frequency histograms. The

final cytogram displays each cell as a single point characterized by two variables, total (Y axis) fluorescence vs alpha t (X axis). In the cytogram, the left-most compact cluster in the shape of a vertical ellipse contains sperm with normal chromatin structure and is termed the ‘main population’ (Evenson, 1999). To the right of this is a second cluster which contains sperm with decreased green fluorescence and increased red fluorescence due to denatured DNA; this population makes up the %COMP α . The computer then generates an alpha t frequency histogram from the data. Since the frequency histogram represents only one parameter (alpha t), it clearly demonstrates the main and the %COMP α populations as peaks instead of points. The histogram is divided into two regions: region 1 includes the SCSA values for the entire sample population and region 2 contains values for %COMP α .

Statistical Analysis

Data were analyzed by the General Linear Models procedure available through SAS®.

The model used for analysis of variance for morphology and post-thaw progressive motility was as follows:

$$Y_{ijk} = \mu + S_i + B_{(i)j} + D_k + e_{ijk}$$

Where Y_{ijk} = percent post-thaw progressive motility or percent primary abnormalities;

μ = the overall mean;

S_i = the fixed effect of the season i (i = Fall or Spring);

$B_{(i)j}$ = the random effect of the bull j within season i (j = 1,2,3. . . 6);

D_k = the fixed effect of the day k (k = D-8, D-5, D-1 . . . D34);

e_{ijk} = random error.

The model used for analysis of variance for the SCSA variables of $\bar{x}\alpha$, $SD\alpha$, and $\%COMP\alpha$ was as follows:

$$Y_{ijk} = \mu + S_i + B_{(i)j} + D_k + R_l + e_{ijk}$$

Where

$$Y_{ijk} = \alpha, SD\alpha, \text{ and } \%COMP\alpha$$

μ = the overall mean;

S_i = the fixed effect of the season i (i = Fall or Spring);

$B_{(i)j}$ = the random effect of the bull j within season i ($j = 1, 2, 3, \dots, 6$);

D_k = the fixed effect of the day k ($k = D-8, D-5, D-1 \dots D34$);

R_l = the fixed effect of the replication j ($j = 1, 2$)

e_{ijk} = random error.

The model used for analysis of variance for the AOA variables of $\%SHIFT$ and $\%SHIFT$ NORMAL was as follows:

$$Y_{ijk} = \mu + S_i + B_{(i)j} + D_k + R_l + e_{ijk}$$

Where

$$Y_{ijk} = \%SHIFT \text{ and } \%SHIFT \text{ NORMAL};$$

μ = the overall mean;

S_i = the fixed effect of the season i (i = Fall or Spring);

$B_{(i)j}$ = the random effect of the bull j within season i ($j = 1, 2, 3, \dots, 6$);

D_k = the fixed effect of the day k ($k = D-8, D-5, D-1 \dots D34$);

R_l = the fixed effect of the replication j ($j = 1, 2$)

e_{ijk} = random error.

Pearson simple correlations were performed on all variables using the CORR procedure of SAS®.

Chapter V.

RESULTS

Efficiency of scrotal insulation in perturbing spermatogenesis may be reduced or exacerbated by ambient conditions. Ambient temperatures were similar between the two seasons in the experiment. Ambient temperatures during the experiment ranged from -3.3°C to 23.3°C during October and November 1999 (collection period 1), and from -2.2°C to 29.4°C during March and April 2000 (collection period 2). The mean high/low ambient temperatures throughout the experiment were $17^{\circ}\text{C}/3.7^{\circ}\text{C}$ and $20.4^{\circ}\text{C}/5.6^{\circ}\text{C}$ for the first and second collection periods, respectively. The mean high/low ambient temperatures during the scrotal insulation period were $20.6^{\circ}\text{C}/9.7^{\circ}\text{C}$ and $19.7^{\circ}\text{C}/7.2^{\circ}\text{C}$ for the first and second collection periods, respectively. (Data provided by the Blacksburg Weather Service). Season did not have a significant effect on the appearance of any primary abnormality or on motility, but it did have an effect on all the variables associated with perturbed chromatin structure ($P < 0.05$) (Tables 1, 2, and 3).

Analysis of variance for all the primary abnormalities quantified are shown in Table 1. Individual bull response and day of collection accounted for the appearance of decaps, apical vacuoles, random vacuoles, pyriforms, and severely misshapen heads ($P < .05$), but not for the appearance of diadems. Figure 1 illustrates the overall shift towards morphologically abnormal cells that were sought in this experiment following the onset of the thermal insult to the testes. This figure shows an increase in both abnormal head conformation and nuclear vacuolizations beginning approximately 13 days after the placement of the scrotal sacks, peaking at days 20 to 23, and tapering down slowly thereafter to the end of the semen collection period (Day 34 post-insult). Figures 2 through 4 illustrate the frequency in appearance of specific abnormalities, expressed as the means ($\pm\text{SE}$) across the six bulls. The deviation from the means that occurs in the post-insult period exemplifies the variation across bulls in response to the thermal insult. Decapitated sperm cells (decaps) (Figure 2A) were the first abnormal cells to appear

Table 1. Analysis of Variance (ANOVA) of Specific Primary Abnormalities Induced by a 48-h Testicular Thermal Insult

Source	df	Decap		Diadem		Apical Vacuole	
		Mean Square	P	Mean Square	P	Mean Square	P
season	1	138.67	0.11	45.39	0.49	306.02	0.08
Bull (season)	4	217.04	0.01	160.21	0.16	365.41	0.01
day	12	165.22	0.00	149.85	0.11	496.81	<0.0001
error	60	53.70		92.86		96.94	

Source	df	Random Vacuole		Pyriform		Severely Misshapen	
		Mean Square	P	Mean Square	P	Mean Square	P
season	1	24.82	0.40	6.78	0.79	0.21	0.94
Bull (season)	4	946.44	<0.0001	593.77	0.00	208.85	0.00
day	12	87.12	0.01	231.89	0.01	82.28	0.02
error	60	34.99		92.37		36.43	

Table 2. ANOVA of Percent Post-Thaw Motility

Source	df	Mean Square	P
season	1	92.42	0.3622
Bull (season)	4	618.58	0.0014
day	7	266.01	0.0394
error	31	108.04	

Table 3. ANOVA of SCSA and AOA Variables

Source	df	X α t		Sdat	
		Mean Square	P	Mean Square	P
season	1	597.19	0.0070	478.26	0.0253
Bull (season)	4	448.9	0.0003	1143.25	<0.0001
replicate	1	3.93	0.8239	0.6	0.9364
day	10	350.73	<0.0001	481.79	<0.0001
error	113	78.99		93.13	

Source	df	%COMP α t		% SHIFT		%SHIFT NORMAL	
		Mean Square	P	Mean Square	P	Mean Square	P
season	1	146.69	0.0100	83209.71	0.0126	6616.01	0.1910
Bull (season)	4	287.22	<0.0001	166959.22	<0.0001	19166.61	0.0011
replicate	1	0.01	0.9864	743.53	0.8099	1487.92	0.5335
day	10	129.04	<0.0001	38625.99	0.0071	4132.58	0.3800
error	113	21.35		12764.64		3804.44	

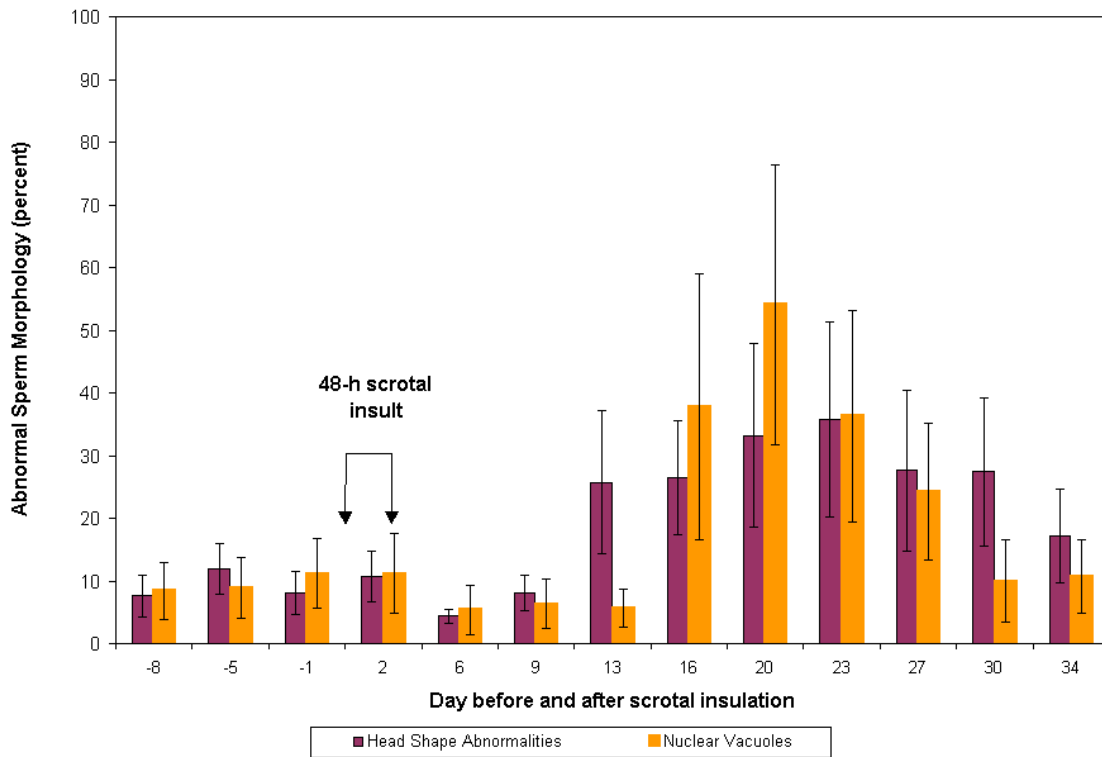


Figure 1. The effects of 48-h scrotal insulation on overall abnormal sperm head morphology and nuclear vacuolization across bulls (n=6). Data represented as means (\pm SE)

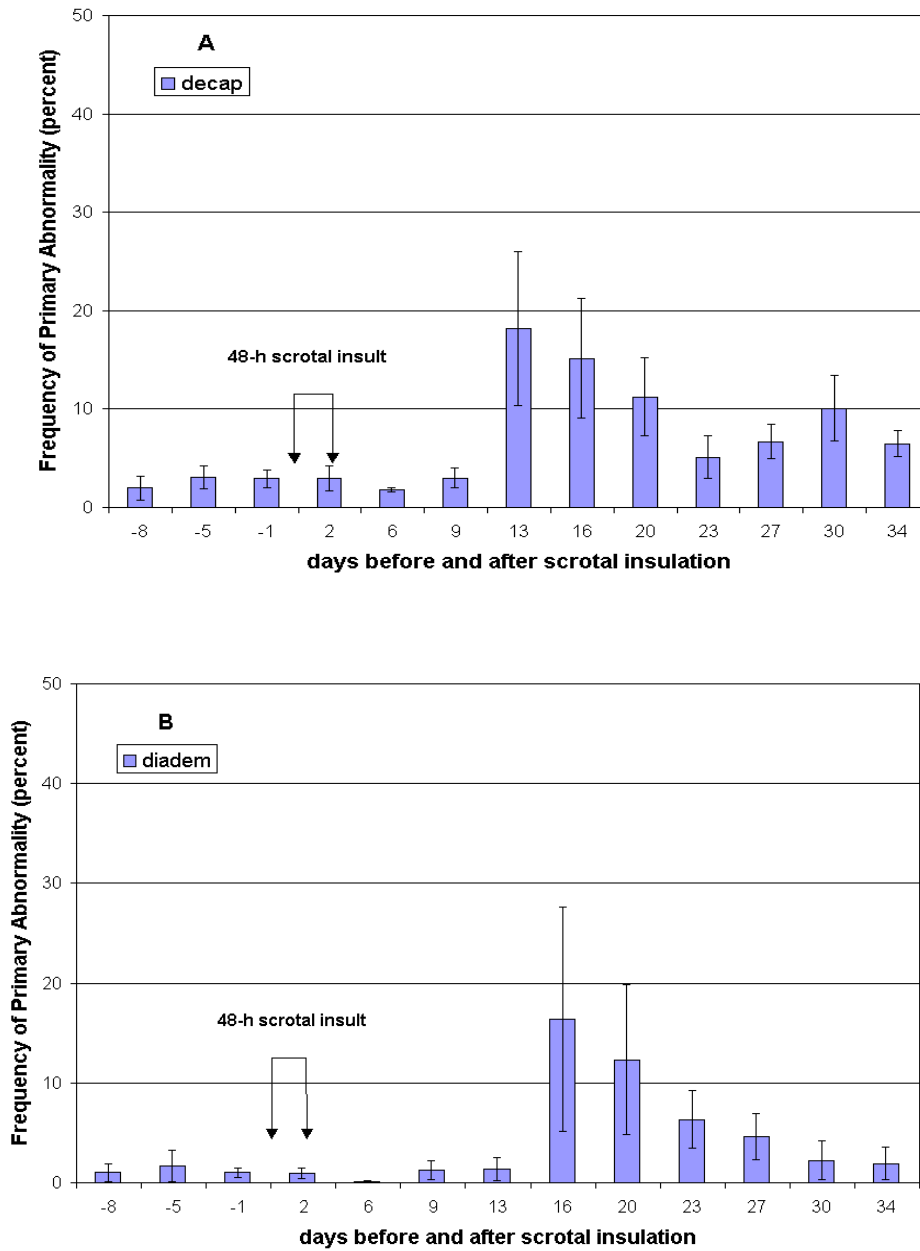


Figure 2. Means (\pm SE) in the percentage of decapitated spermatozoa (A) and diadem defect (B) in relation to the 48-h scrotal insult across all bulls (n=6)

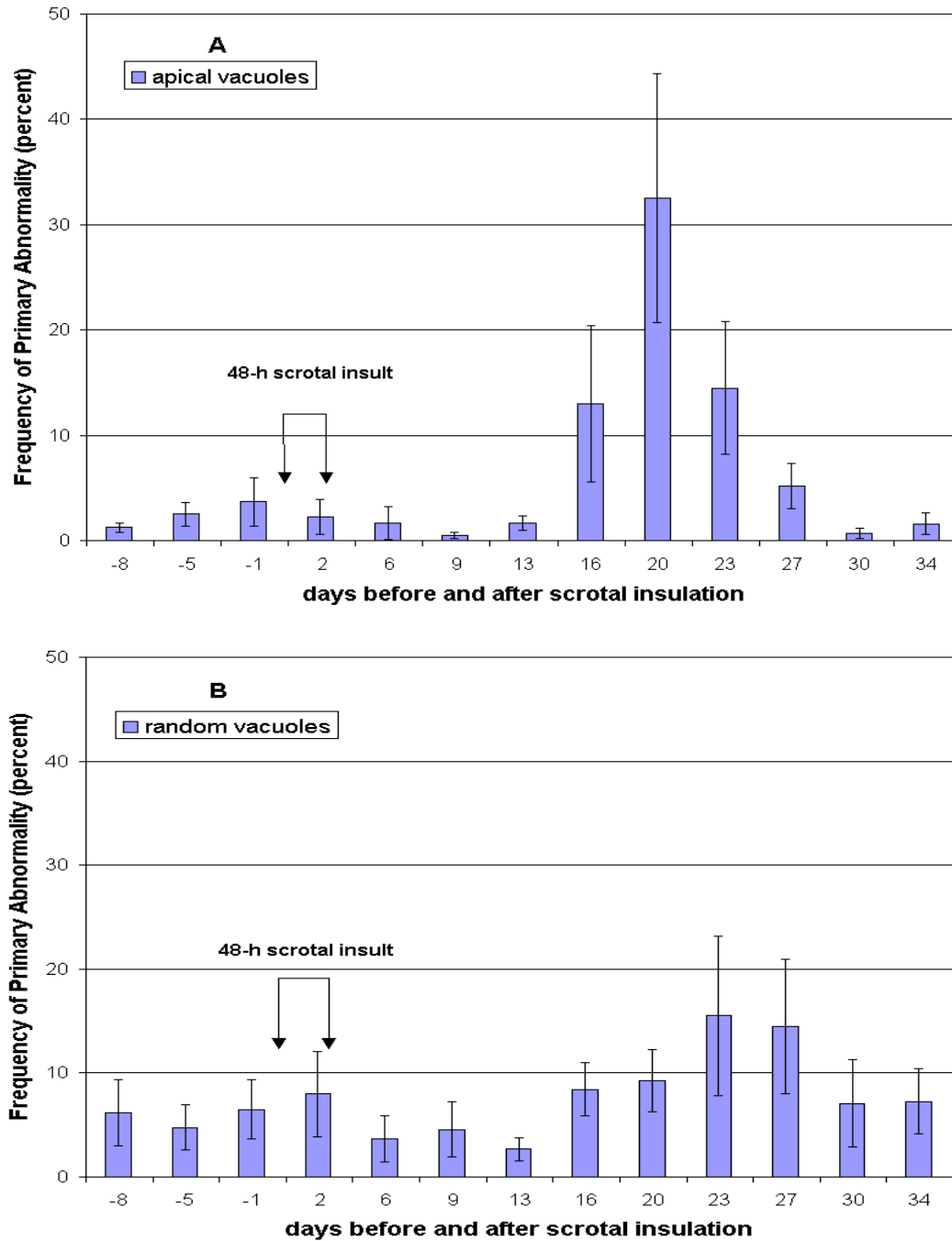


Figure 3. Means (\pm SE) in the percentage of apical vacuoles (A) and random vacuoles (B) in relation to the 48-h scrotal insult across all bulls (n=6)

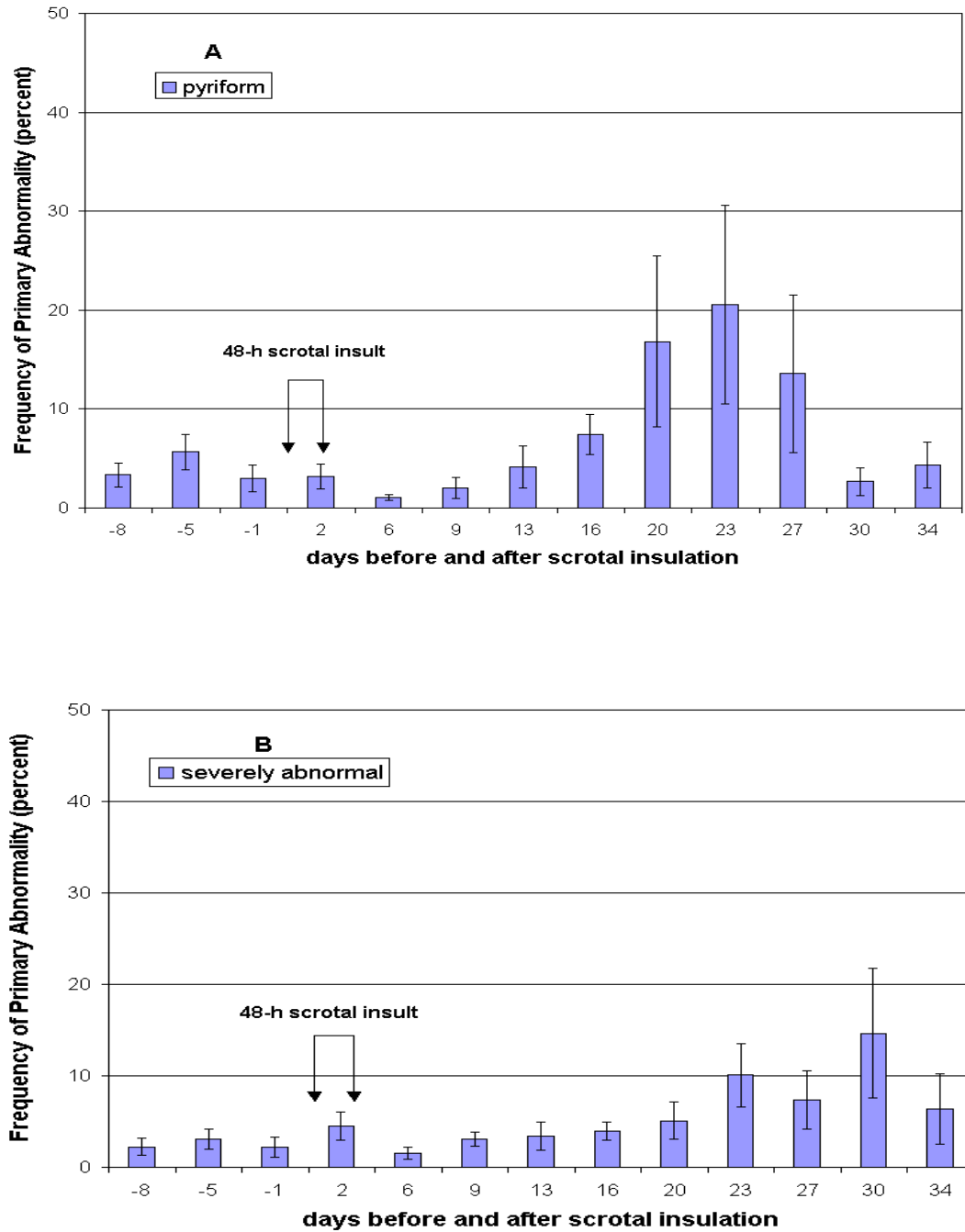


Figure 4. Means (\pm SE) in the percentage of pyriform (A) and severely abnormal spermatozoa (B) in relation to the 48-h scrotal insult across all bulls (n=6)

after the scrotal insult (Day 13), followed by the appearance of diadems (Figure 2B) and apical vacuoles (Figure 3A) on Day 16 post-insult. Random vacuoles (Figure 3B) appeared along with diadems and apical vacuoles, but tended to continue to rise along with the appearance of pyriform heads (Days 20 to 23; Figure 4A). Spermatozoa with severely abnormal heads appeared on Day 23 and peaked on Day 30 (Figure 4B).

The effects of the mild scrotal insulation on the appearance of primary abnormalities for each bull are represented in Figures 5 through 10. More specifically, these figures demonstrate the great variation among the bulls in their response to the thermal insult as revealed in the percentage of abnormal spermatozoa in their ejaculates. Bulls A, B, C, and D displayed sperm having distinct increases in nuclear vacuolization in the days following the thermal insult, whereas bulls E and F did not show an apparent increase in vacuolization. Bull D is unique among the bulls in that he is the only male that showed a very marked increase in diadem and apical vacuoles (71% and 45%, respectively) on Day 16 post-insult, without a marked increase in any other primary abnormality on that day. In terms of an overall increase in morphological aberrations due to the thermal stress, Bulls A and B were the highest responders, bulls C and D were intermediate responders, and bulls E and F were low responders. However, it is important to note that bull D (Figure 8) had the single highest percentage increase in diadems of any bull on any given day; this will prove useful in understanding the relationship of the diadem defect to chromatin structure stability.

Significant correlations (Table 4) existed between the appearance of pyriforms and both apical vacuoles and diadems ($r = 0.56$, $r = 0.40$; $P < .01$), and between the appearance of pyriforms and random vacuoles and severely abnormal spermatozoa ($r=0.54$, $r = 0.47$; $P < .01$). There was no significant correlation between the appearance of decapitated spermatozoa and any form of vacuolization.

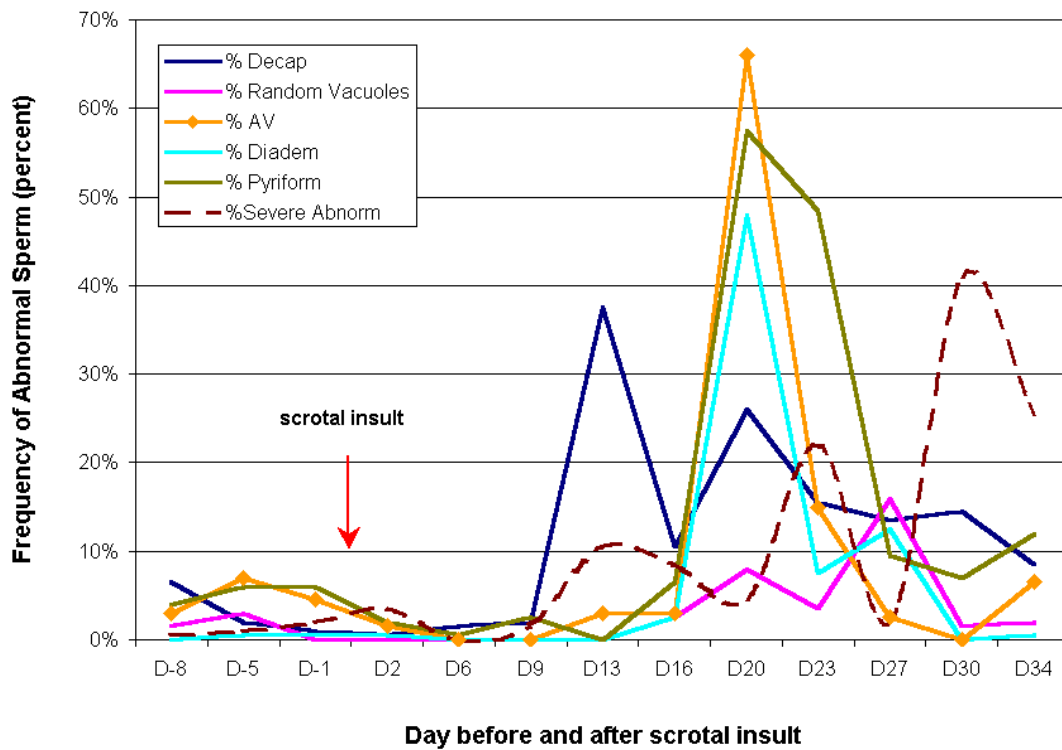


Figure 5. Response of Bull A to 48-h scrotal insulation based on the appearance of specific abnormal cell types in the ejaculate. Bull A is an overall high responder in terms of an overall increase in morphological aberrations due to the thermal stress. (AV= apical vacuoles; diadem= diadem vacuoles)

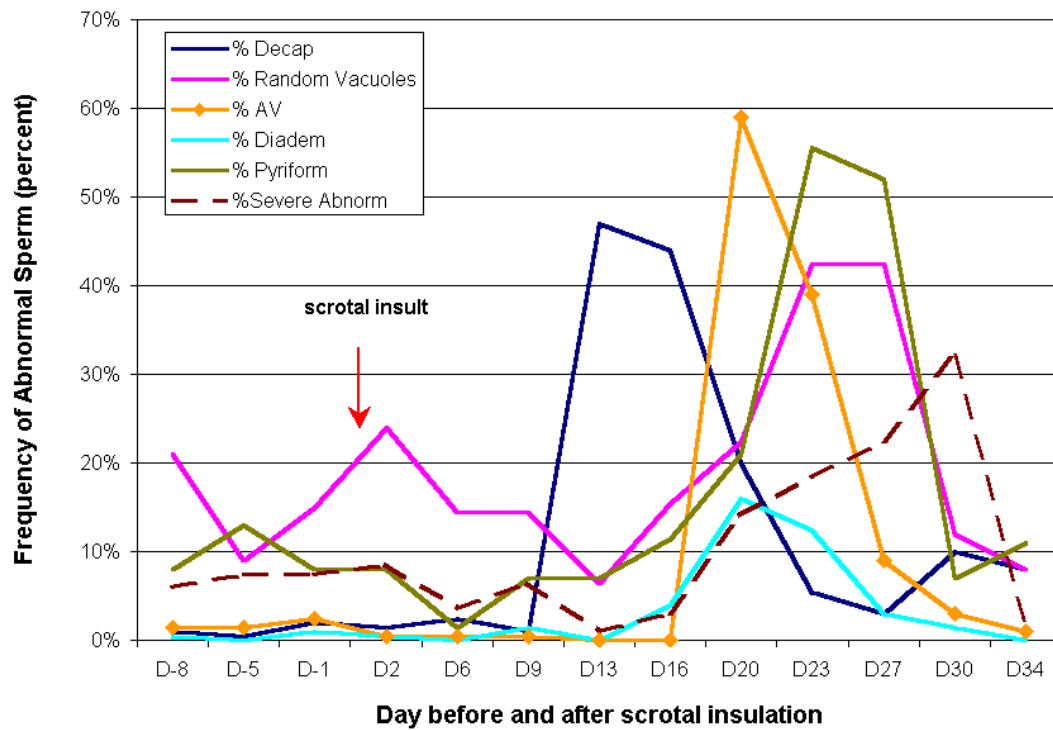


Figure 6. Response of Bull B to 48-h scrotal insulation based on the appearance of specific abnormal cell types in the ejaculate. Bull B is also an overall high responder in terms of an overall increase in morphological aberrations due to the thermal stress. (AV= apical vacuoles; diadem= diadem vacuoles)

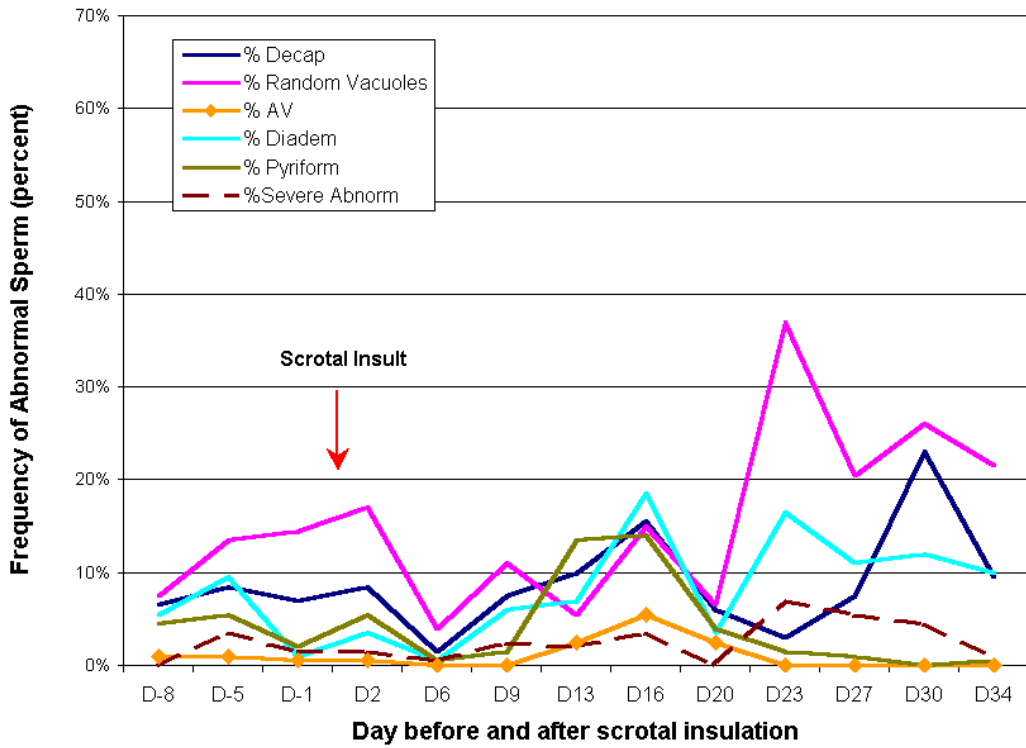


Figure 7. Response of Bull C to 48-h scrotal insulation based on the appearance of specific abnormal cell types in the ejaculate. Bull C is a moderate responder in terms of an overall increase in morphological aberrations due to the thermal stress. (AV= apical vacuoles; diadem= diadem vacuoles)

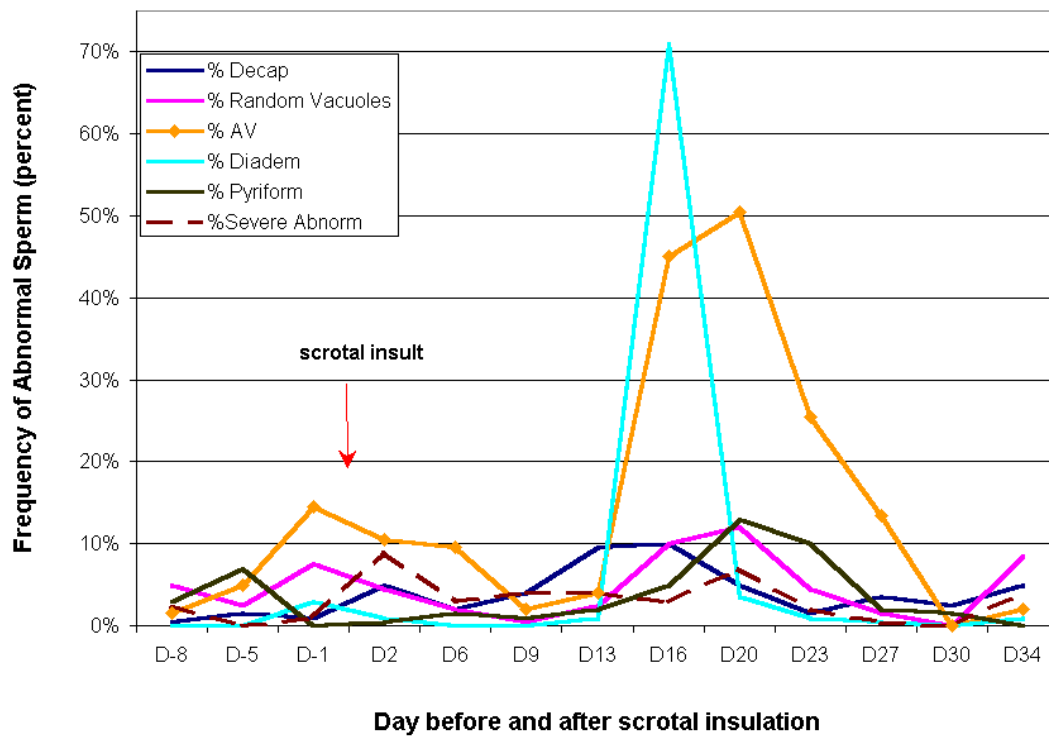


Figure 8. Response of Bull D to 48-h scrotal insulation based on the appearance of specific abnormal cell types in the ejaculate. Bull D is a unique moderate responder because of a marked appearance of the diadem defect and apical vacuoles in the absence of misshapen heads. In addition, this degree of response measured in terms of an overall increase in morphological aberrations due to the thermal stress. (AV= apical vacuoles; diadem= diadem vacuoles)

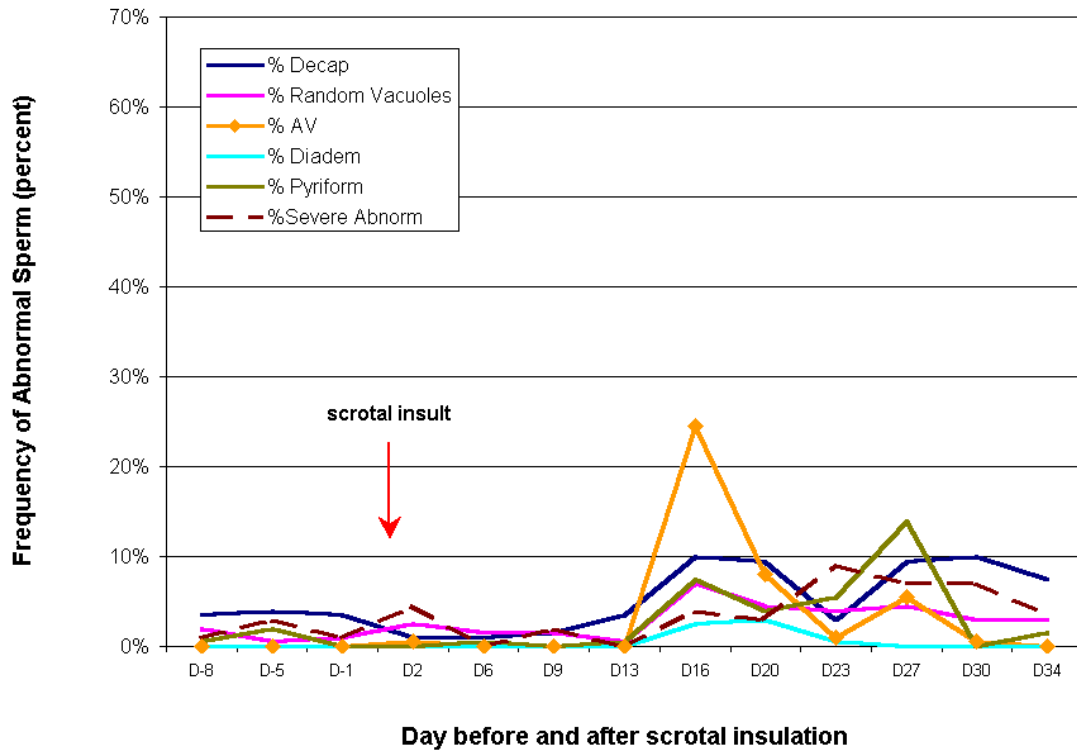


Figure 9. Response of Bull E to 48-h scrotal insulation based on the appearance of specific abnormal cell types in the ejaculate. Bull E is a low responder in terms of an overall increase in morphological aberrations due to the thermal stress. (AV= apical vacuoles; diadem= diadem vacuoles)

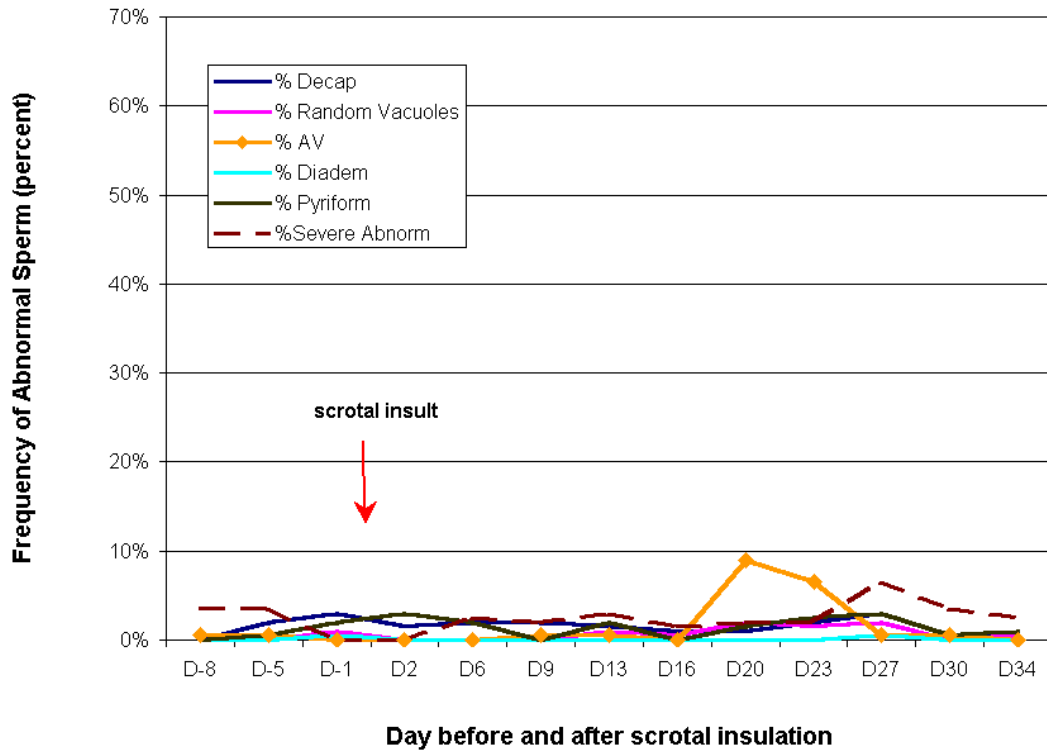


Figure 10. Response of Bull F to 48-h scrotal insulation based on the appearance of specific abnormal cell types in the ejaculate. Bull F is the lowest responder in terms of an overall increase in morphological aberrations due to the thermal stress. (AV= apical vacuoles; diadem= diadem vacuoles)

Table 4. Correlation Coefficients (r values): Associations between Specific Primary Abnormalities and Motility

Variable	random vacuole	apical vacuole	diadem	pyriform	severely abnormal	% motility
decap ¹	0.14	0.21	0.23	0.27	0.07	(-)0.46**
random vacuole ¹	1.00	0.20	0.23	0.54**	0.41**	(-)0.37*
apical vacuole ¹		1.00	0.66**	0.56**	0.23	(-)0.32*
diadem ¹			1.00	0.40**	(-)0.01	(-)0.31*
pyriform ¹				1.00	0.47**	(-)0.67**
severely abnormal ¹					1.00	(-)0.40**
normal/subtly misshapen ¹						0.74**
* P <0.05						
** P<0.01						
¹ N=48						
² N=44						

Table 5. Correlation Coefficients (r values): Relationship between Chromatin Structure Assay Variables (SCSA and AOA) and Abnormal Morphology and Motility

Variable	X _{αt}	SD _{αt}	%COMP _{αt}	%SHIFT	%SHIFT NORMAL
decap ¹	0.36*	0.30*	0.51**	0.52**	0.44**
random vacuole ¹	0.50*	0.40**	0.42**	0.44**	0.39**
apical vacuole ¹	0.15	0.14	0.21	0.26	(-)0.01
diadem ¹	0.16	0.14	0.19	0.23	(-)0.01
pyriform ¹	0.43**	0.47**	0.48**	0.61**	0.18
severely abnormal ¹	0.36*	0.52**	0.38**	0.43**	0.28*
% Motility ²	(-)0.52**	(-)0.55**	(-)0.67**	(-)0.68**	(-)0.26
* P <0.05					
** P<0.01					
¹ N=48					
² N=44					

Table 6. Correlation Coefficients (r values): Associations Between Chromatin Structure Assay Variables (SCSA and AOA)

Variable	SD _{αt}	%COMP _{αt}	%SHIFT	%SHIFT NORMAL
X _{αt} ³	0.91**	0.92**	0.74**	0.42**
SD _{αt} ³	1.00	0.88**	0.75**	0.40**
%COMP _{αt}		1.00	0.84**	0.49**
%SHIFT ³			1.00	0.72**
%SHIFT NORMAL ³				1.00
* P <0.05				
** P<0.01				
³ N=47				

The analysis of variance for percent post-thaw motility shows that, as with the morphology, individual bull response and day of collection influenced the variation in percent motility across the collection period ($P < 0.05$; Table 2). Overall percent post-thaw motility averaged across the bulls decreased approximately 10 percentage points between Day 13 and Day 16 post-insult (62% and 52%, respectively), and dropped to the lowest value, 47%, on Day 27 of collection (Figure 11). Percent motility was negatively correlated (Table 4) with the appearance of pyriforms ($r = -0.67$; $P < 0.01$), decaps ($r = -0.46$; $P < 0.01$), severely abnormal ($r = -0.40$; $P < 0.01$), random vacuoles ($r = -0.37$; $P < .05$), apical vacuoles ($r = -0.32$; $P < .05$), and diadems ($r = -0.31$; $P < .05$).

Analysis of variance for the AOA variables %SHIFT and %SHIFT NORMAL quantified are shown in Table 3. Individual bull response had the most significant effect on %SHIFT ($P < 0.01$) and %SHIFT NORMAL ($P < 0.01$). Day of collection ($P < 0.01$) also accounted for the %SHIFT, but the sample replicates did not account significantly for variation associated with %SHIFT (Table 3).

Analysis of variance for the SCSA variables $\bar{x}\alpha$, $SD\alpha$, and %COMP α are shown in Table 3. Day of Collection had the most significant overall effect on all three SCSA variables ($P < 0.01$), and individual bull response also had a significant effect on $SD\alpha$ ($P < 0.01$), %COMP α ($P < 0.01$) and $\bar{x}\alpha$ ($P < 0.01$).

The relationships between sperm morphology and motility with nuclear chromatin stability measured through the use of both fluorescence microscopy (AOA) and flow cytometry (SCSA) are presented as correlation coefficients (Table 5). Also, Figures 12 through 14 show the relationship between thermally induced primary abnormalities and the percentage of cells that shifted from green fluorescence for each bull based on %SHIFT (AOA) and %COMP α (SCSA). The AOA parameter of %SHIFT represents the total percentage of cells in the sample that showed chromatin denaturation and was highly correlated with the appearance of pyriforms in the ejaculate ($r = 0.61$; $P < 0.01$).

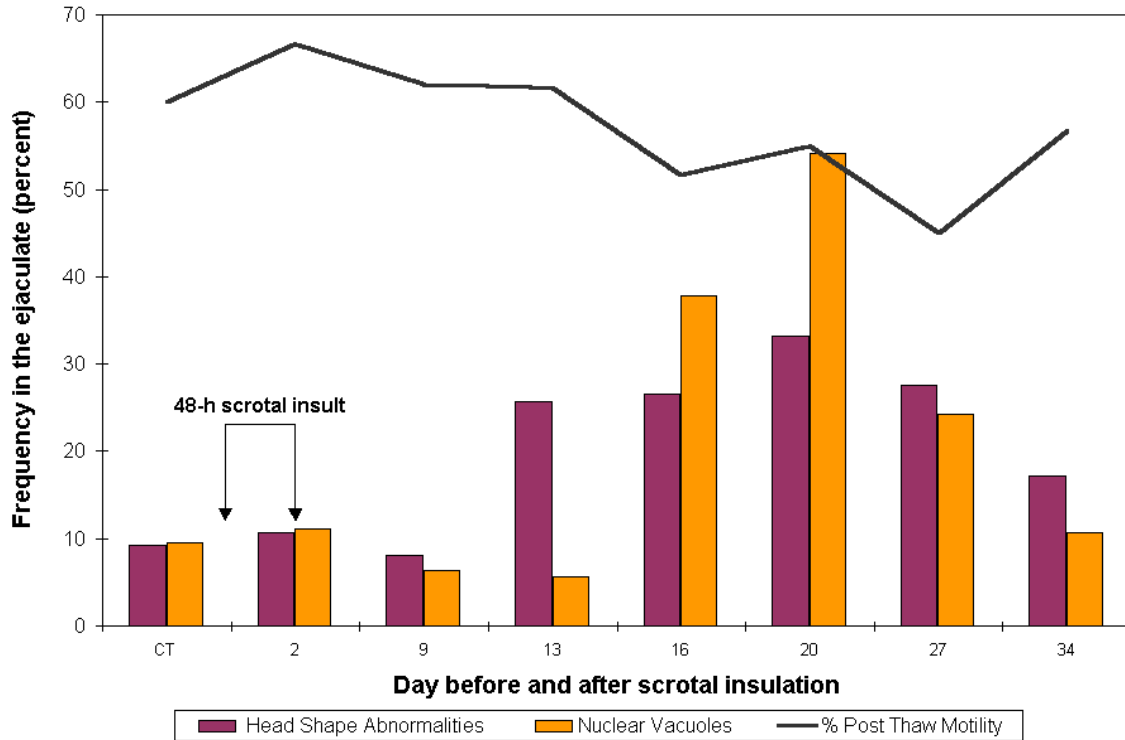


Figure 11. The relationship between the percent of total primary abnormalities and the percent motility across all bulls (n=6) throughout the collection period. CT(control period) consists of days -8, -5, and -1.

Percent SHIFT was also highly correlated with the appearance of decaps ($r = 0.52$; $P < 0.01$), random vacuoles ($r = 0.44$; $P < 0.01$), and severely abnormal heads ($r = 0.43$; $P < 0.01$). The AOA parameter of % SHIFT NORMAL, which denotes the percentage of normally-shaped heads displaying chromatin denaturation, was highly correlated with the appearance of decaps ($r = 0.44$; $P < 0.01$), random vacuoles ($r = 0.39$; $P < 0.01$), and severe abnormalities ($r = 0.28$; $P < 0.05$). Neither diadems nor apical vacuoles were correlated with % SHIFT, suggesting that the appearance of these specific vacuolizations does not indicate a disturbance in the chromatin condensation of the nucleus. This is best exemplified by bull D, who had the single highest percentage increase in diadems of any bull (71%) on Day 16 yet showed a decrease to near baseline (0.8%) in % SHIFT on the same sample (Figure 13). As important, percent post-thaw motility was negatively correlated to the percentage of cells exhibiting a shift towards nuclear denaturation ($r = -0.68$; $P < 0.01$).

All three SCSA variables, $X\alpha$, $SD\alpha$, and $\%COMP\alpha$, were correlated to the appearance of decaps, random vacuoles, pyriforms, and severely abnormal heads (at least $P < 0.05$) but $\%COMP\alpha$ displayed the highest degree of correlation ($P < 0.01$) with most of the aforementioned abnormalities (Table 5). Percent post-thaw motility was also negatively correlated to $\bar{x}\alpha$ ($r = -0.52$; $P < 0.01$), $SD\alpha$ ($r = -0.55$; $P < 0.01$), and $\%COMP\alpha$ ($r = -0.67$; $P < 0.01$) (Table 5).

Correlations were assessed between the AOA and SCSA variables to determine if a relationship existed between the two assays in their ability to discern sperm chromatin structure instability (Table 6). The AOA variable %SHIFT was highly correlated ($P < 0.01$) to all three of the SCSA variables $X\alpha$ ($r = 0.74$), $SD\alpha$ ($r = 0.75$), and $\%COMP\alpha$ ($r = 0.84$). Clearly, % SHIFT (AOA) and $\%COMP\alpha$ (SCSA) were the most

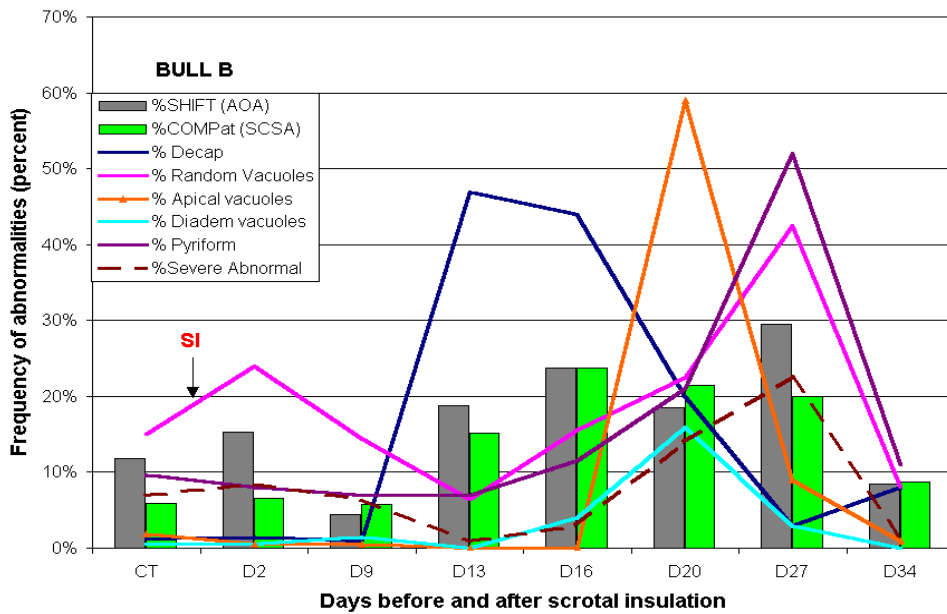
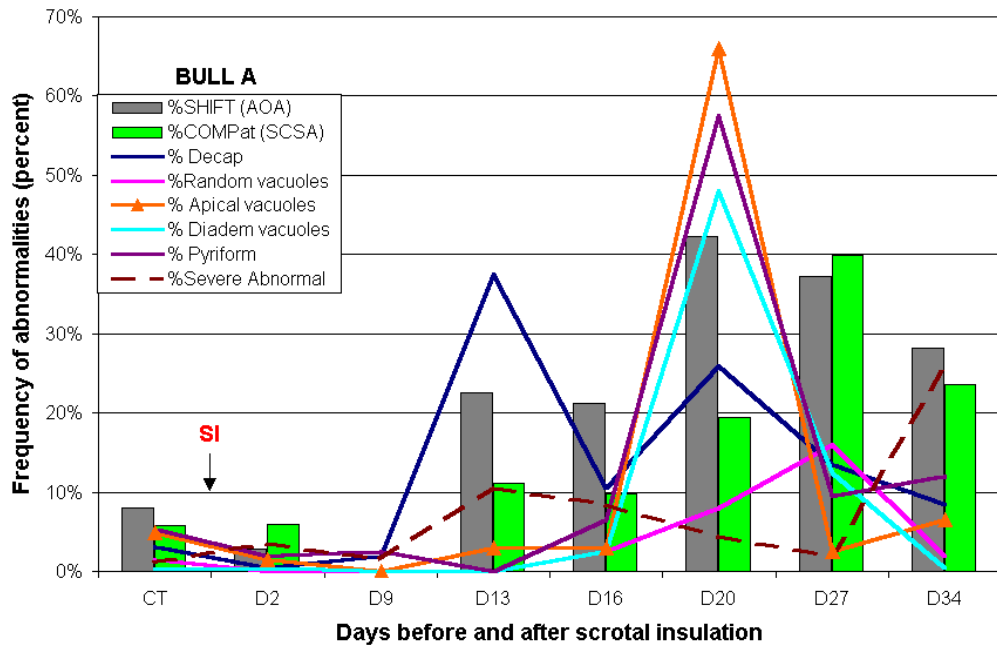


Figure 12. The relationship between the changes in chromatin structure represented by %COMPat (SCSA) and %SHIFT (AOA) and the appearance of specific primary abnormalities induced by the 48-h scrotal insulation in bulls A and B.

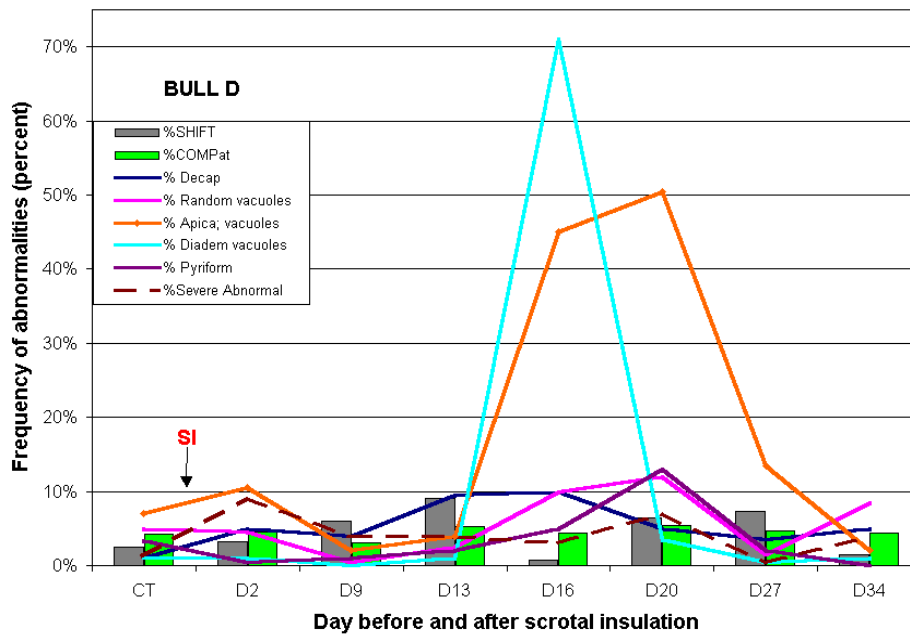
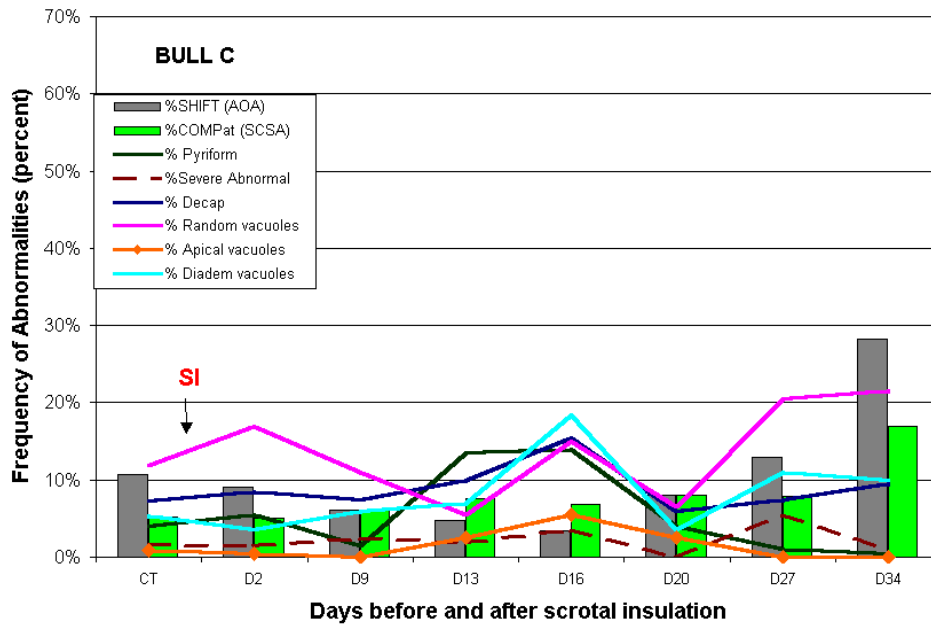


Figure 13. The relationship between the changes in chromatin structure represented by %COMPat (SCSA) and %SHIFT (AOA) and the appearance of specific primary abnormalities induced by the 48-h scrotal insulation in bulls C and D.

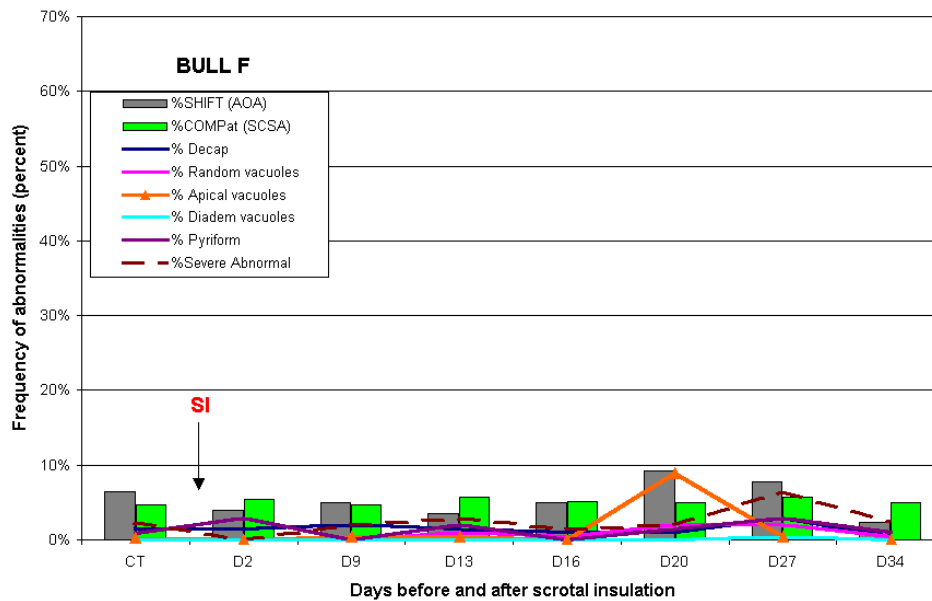
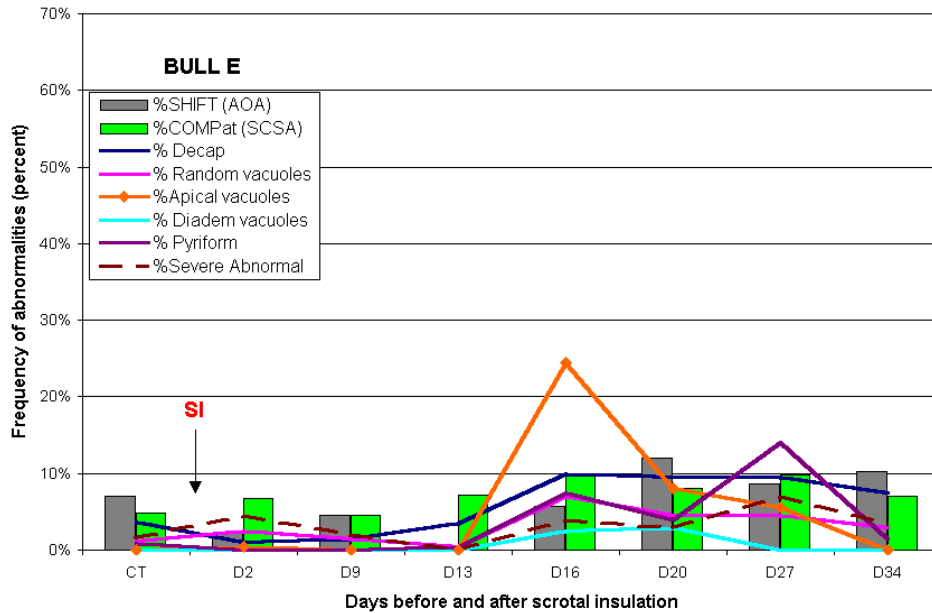


Figure 14. The relationship between the changes in chromatin structure represented by %COMP α (SCSA) and %SHIFT (AOA) and the appearance of specific primary abnormalities induced by the 48-h scrotal insulation in bulls A and B. highly related variables. Figures 12 through 14 graphically display the relationship between %COMP α (SCSA) and %SHIFT (AOA) as they relate to the appearance of specific primary abnormalities for each bull across the collection period. It is apparent

that %COMP α and %SHIFT are highly reflective of each other, as also indicated by their overall correlation of $r = 0.84$ (Table 6).

The repeatability of the replicates also determines the accuracy and strength of an assay. The correlation between % SHIFT replicates was ($r = 0.65$; $P < 0.01$), while the correlations between X α , SD α , and %COMP α replicates were ($r = 0.86$; $P < 0.01$), ($r = 0.87$; $P < 0.01$), and ($r = 0.98$; $P < 0.01$) respectively (data not shown).

Examples of SCSA-generated data for highest and lowest responding bulls are presented as scattergrams and histograms in Figures 15 and 16. Representative digital images of AOA treated sperm cells are shown in Figures 17 and 18 to demonstrate the difference in fluorescence staining between highest and lowest responding bulls.

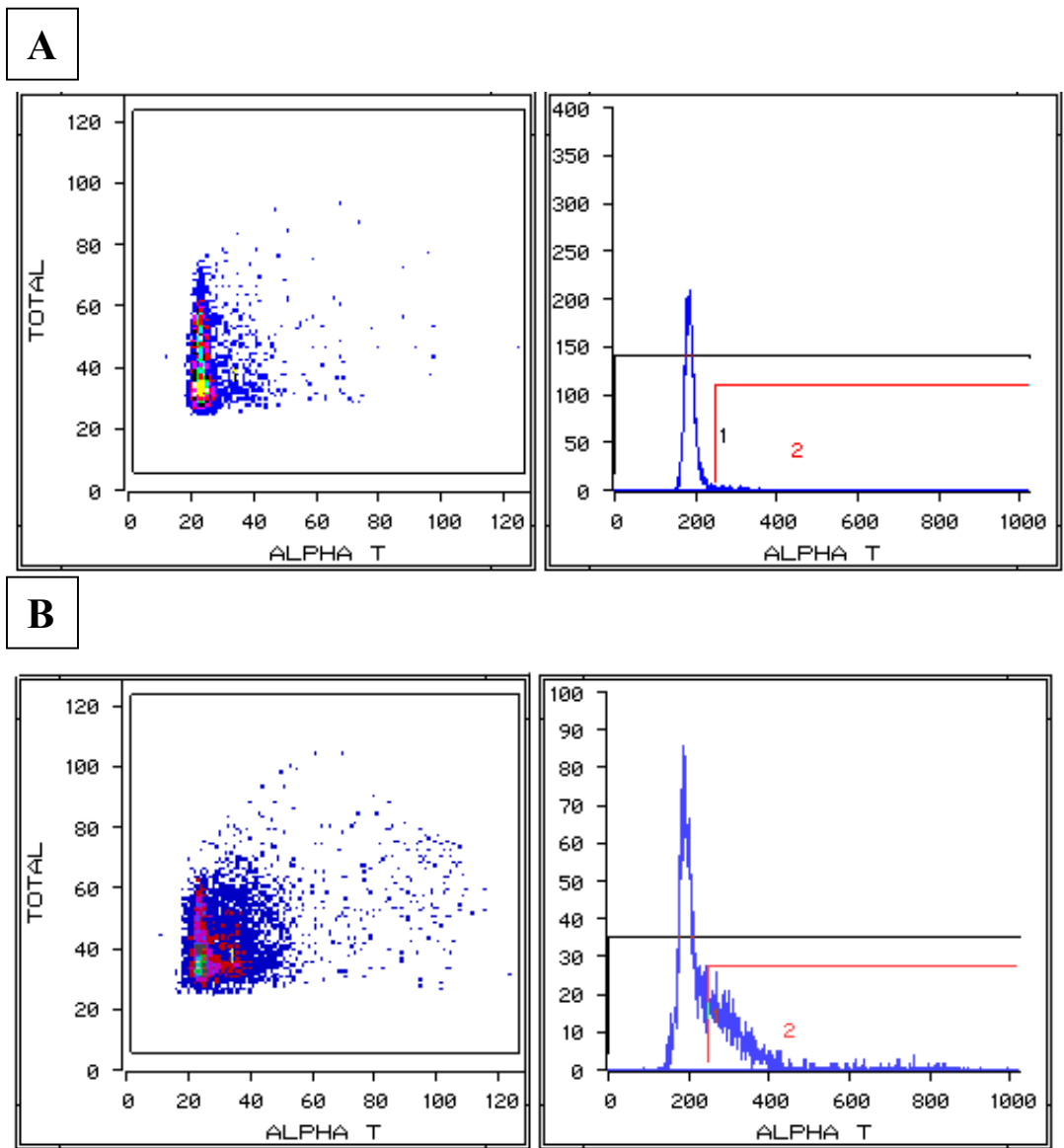


Figure 15. Scattergram and histogram representations of SCSA data for Bull A (highest responder) on A) control pre-insult semen sample and B) Day 27 post-insult semen sample. (Left panel) The raw data for each cell is calculated as ‘alpha t’ (αt), or the ratio of red fluorescence/[red+green] fluorescence. As a ratio, the main population is represented by the vertical pattern in the scattergram. The Y axis is total fluorescence (red+green) and the X axis is αt . The %COMP α population falls outside of the main vertical pattern. (Right panel) The computer-calculated frequency histogram of αt shows both populations more clearly. Region 1 includes the SCSA values for the whole sample population; region 2 contains values for %COMP α .

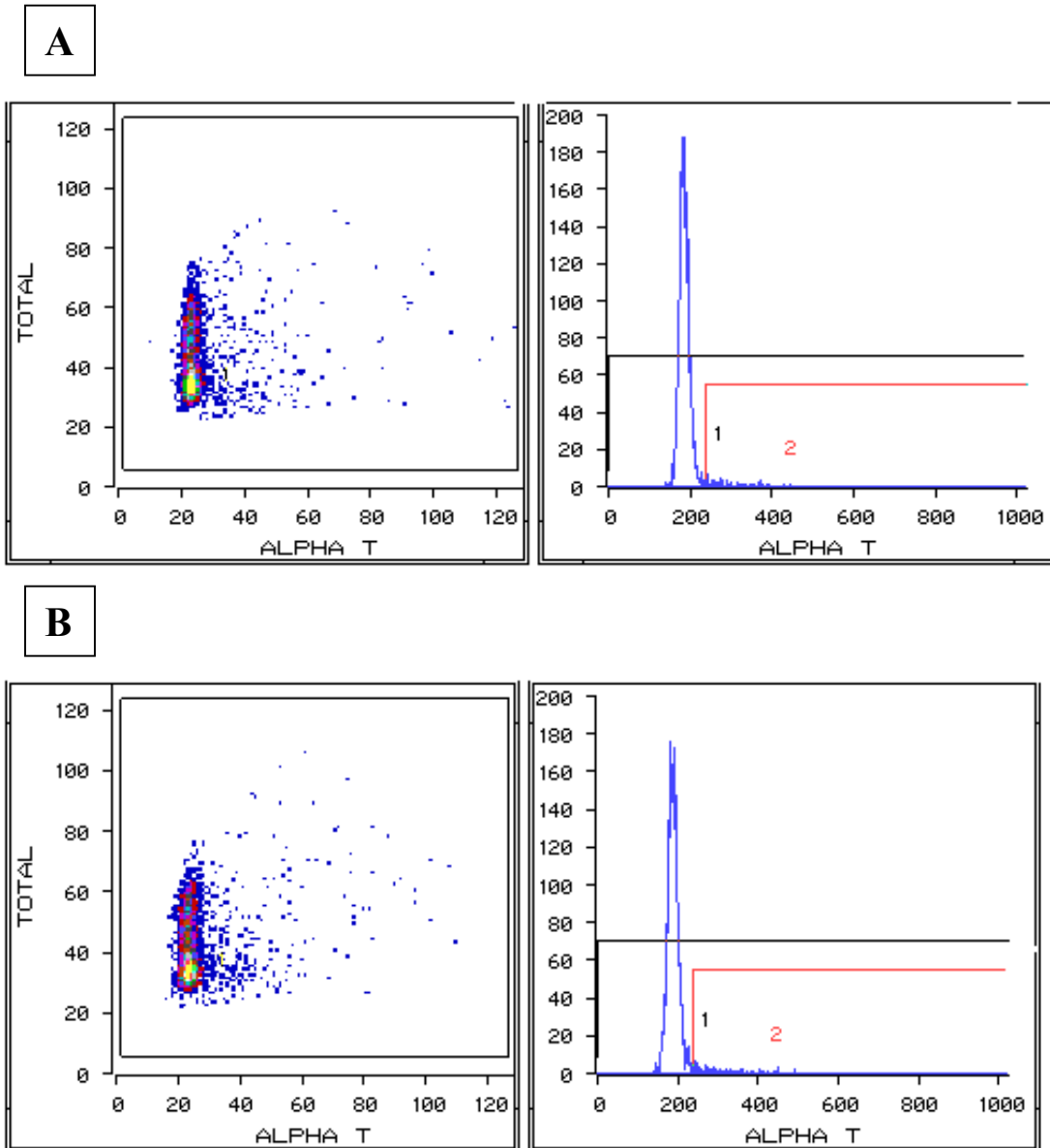
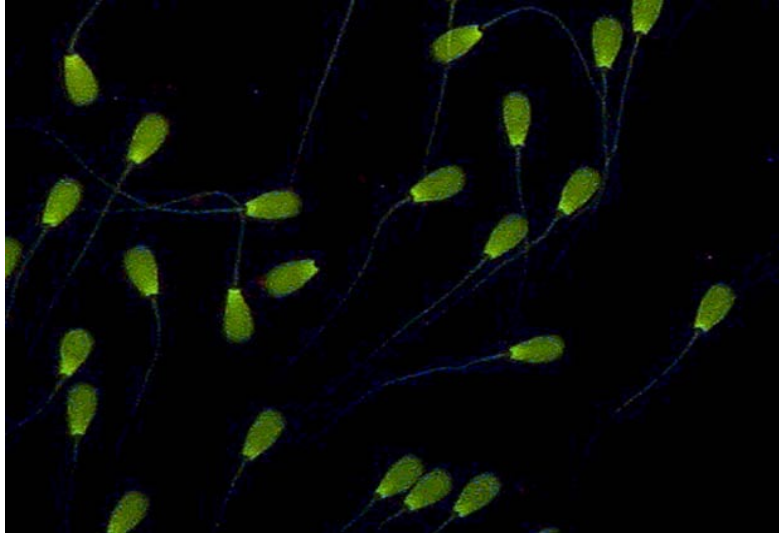


Figure 16. Scattergram and histogram representations of SCSA data for Bull F (lowest responder) on A) control pre-insult semen sample and B) Day 27 post-insult semen sample. (*Left panel*) The raw data for each cell is calculated as ‘alpha t’ (αt), or the ratio of red fluorescence/[red+green] fluorescence. As a ratio, the main population is represented by the vertical pattern in the scattergram. The Y axis is total fluorescence (red+green) and the X axis is αt . The %COMP αt population falls outside of the main vertical pattern. (*Right panel*) The computer-calculated frequency histogram of αt shows both populations more clearly. Region 1 includes the SCSA values for the whole sample population; region 2 contains values for %COMP αt .

a



b

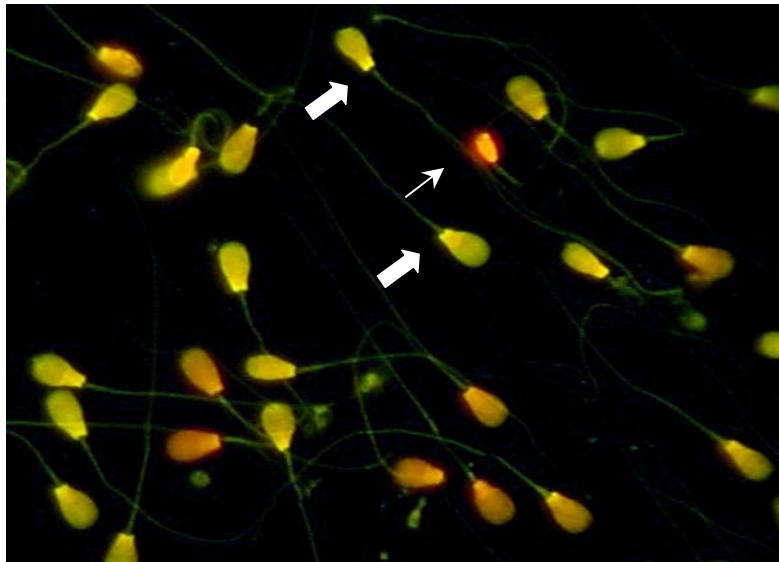


Figure 17. Digital images representing AOA data for Bull A (highest responder) on a) control pre-insult semen sample and b) Day 27 post-insult semen sample. All the cells depicted in the control sample (a) fluoresced green, demonstrating a resistance to *in situ* acid denaturation. The cells in the Day 27 post-insult (b) sample show a variation in fluorescence color among the cells. Thick arrows denote cells that have undergone slight chromatin denaturation and fluoresce yellow. Thinner arrows denote cells that have undergone more severe chromatin denaturation and fluoresce pink to red. All cells that show a shift from green fluorescence become part of the %SHIFT population.

a



b

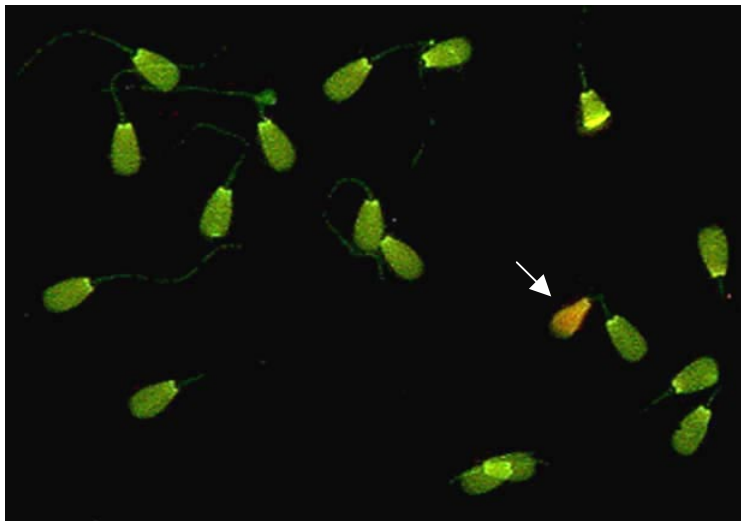


Figure 18. Digital images representing AOA data for Bull F (lowest responder) on a) control pre-insult semen sample and b) Day 27 post-insult semen sample. All the cells depicted in the control sample (a) fluoresced green, demonstrating a resistance to *in situ* acid denaturation. The cells in the Day 27 post-insult (b) sample show very little variation in fluorescence color among the cells, demonstrating an overall resistance to *in situ* acid denaturation. The thin arrow represents a cell that has undergone severe chromatin denaturation and fluoresces red. All cells that show a shift from green fluorescence become part of the %SHIFT population.

Chapter VI.

DISCUSSION

The relationship between post-thaw motility and the chronological appearance of primary abnormalities in this study is in agreement with the previous study of Vogler et al. (1993). Averaged across bulls, post-thaw motility values decreased slightly following the scrotal insulation period, which coincided with the rise in abnormal cells after day 13 post-insult. It is evident that the type, order, and duration of a particular sperm abnormality are reflective of the stage of the cycle of the seminiferous epithelium that the cells were in at the time of scrotal insulation. Amann (1962) described the cycle of the seminiferous epithelium in the bovine as an 8-stage, 13.5-day cycle. Taking into account that rete and epididymal transit of spermatozoa takes approximately 8 to 11 days in bulls (Johnson, 1994) our results suggest that the mild thermal stress interferes with the spermatogenic process. Decapitated heads begin to appear 13 days after the insult, suggesting errors in the implantation socket just prior to spermiation; these early appearing decapitated cells were otherwise normal in appearance. The diadem defect, characterized by a row of vacuoles across the nuclear ring of the sperm head, appeared transiently between days 16 and 20 post-insult. This defect suggests a deficiency in chromatin condensation during stages V through VII of the cycle that was induced after the sperm head shape was set. Apical vacuoles, characterized by a single vacuole on the apical ridge of the sperm head, appear alongside the diadem defect, but tend to persist until day 23 post-insult. Random vacuoles appeared over a greater span of time than the diadem defect or the apical vacuoles, peaking between day 23 through 27. The appearance of the random vacuoles coincided with the appearance of pyriform and severely misshapen heads. The appearance of these defects correspond with stages I through IV of the spermatogenic cycle in which round spermatids are elongating; these stages are highly vulnerable to alterations in sperm head shape and DNA condensation throughout the nucleus. It is also a time when arginine and thiol rich protamines are substituted for the histones in the spermatid, a process considered very important to sperm nuclear condensation and head shape (Sakkas et al., 1995).

As demonstrated in earlier studies, the six bulls in this experiment responded with varying degrees of morphological aberrations to the same 48-h scrotal insulation (Vogler et al., 1993). Scrotal surface temperature was not measured, but previous work using the same insulating materials indicates that scrotal surface temperature increases from 33°C directly after scrotal insulation to 36°C after removal of scrotal sack (Vogler et al., 1993). Bulls A and B were the highest responders, bulls C and D were moderate responders, and bulls E and F were the lowest responders (Figures 5 through 10). This bull variation provided a model for evaluating the sperm chromatin structure stability of morphologically perturbed or intact spermatozoa generated after a mild thermal insult to the testes. The purpose of this model was to determine if the evaluation of sperm chromatin structure was necessary for elucidating sperm characteristics that cannot be classified through the current indicators for disturbed spermatogenesis, namely reduced motility and altered morphology.

The modified chromatin structure assay (AOA) values that denote an increase in chromatin denaturation (%SHIFT and %SHIFT NORMAL) were highly correlated ($P < 0.01$) to the SCSA variables of $\bar{x}\alpha$, $SD\alpha$, and %COMP α (Table 6). The highest correlation occurred between the AOA variable of %SHIFT and the SCSA variable of %COMP α ($r = 0.84$); this relationship is shown graphically in figures 12 through 14. As important, the repeatability of the AOA assay is similar to the repeatability of SCSA on independently measured samples, as noted by the significant correlation between sample replicates for each variable measured. The statistically significant relationship between the AOA variables, SCSA variables, and their respective replicate repeatability strengthens the validity of the AOA technique in assessing chromatin stability in bull spermatozoa.

Both variables %SHIFT and %COMP α were highly correlated with the chronological appearance of decapitated, pyriform, severely abnormal, and randomly vacuolated spermatozoa. The appearance of decapitated sperm induced by the heat did not occur until day 13 after the scrotal insulation, and this suggests that sperm in the epididymis at the time of the insult (represented by sperm collected on days 2 through 9 post-insult) did not undergo a measurable perturbation in chromatin condensation detectable by either AOA or SCSA measurements. This is in contrast to the results of

Karabinus et al. (1997) that show a significant increase in %COMP α in sperm collected before day 9 post-insult.

As important, AOA analysis showed that a proportion of the sperm that exhibited chromatin denaturation were normal in shape (% SHIFT NORMAL). These cells were highly correlated with the appearance of decaps and random vacuoles ($P < 0.01$), as well as severe abnormal (P<0.05), and were most prominent in populations of morphologically abnormal sperm post-insult. These results suggest that damage to chromatin integrity extends beyond morphologically perturbed spermatozoa following a testicular thermal insult and may account for incompetent fertilizing sperm where embryogenesis is impaired (Setchell, 1998).

In the present study, Bull D provided a unique response from the other bulls to the scrotal insult, as shown by the marked increase in diadem defect and apical vacuoles on otherwise morphologically normal sperm (Figure 8, day 16). Saacke et al. (1994) found that sperm with random nuclear vacuoles and diadem defects resulting from a 48-hour scrotal insulation significantly increased the numbers of degenerate, and fair-poor embryos at the expense of excellent to good embryos, when compared to sperm collected prior to the thermal insulation period. Interestingly, neither %SHIFT or %COMP α were correlated with the appearance of diadems, suggesting that this defect does not indicate a perturbation in chromatin condensation of the nucleus.

Nuclear vacuoles are formed by the invagination of the nuclear membrane into the nucleoplasm during spermiogenesis and they are firmly positioned as chromatin condensation is completed (Barth and Oko, 1989). Perhaps the presence of these vacuoles does not affect the proper condensation of chromatin in terms of protamine deposition and disulfide linkage formation, but rather cause a physical hindrance in the arrangement of the chromatin strands on the nuclear matrix. The chromatin strands are organized into specific DNA loop domains that have a specific spatial relationship with the sperm nuclear matrix (Ward and Coffey, 1991). Somatic cell DNA replication occurs at specific sites on the nuclear matrix, and the specific spatial relationship between DNA loop domains and the nuclear matrix in sperm suggests that specific sites for replication also exist on the sperm nuclear matrix (Stief et al., 1989). McCarthy and Ward (2000) have shown that the structural integrity of the sperm nuclear matrix may be necessary for

the proper unpackaging of sperm DNA for participation in embryogenesis. Therefore, severe nuclear vacuolization in otherwise morphologically normal sperm that can undergo fertilization may result in embryonic degeneration because of an inactivation or mutation of paternal genes through improper association with the sperm nuclear matrix.

The overall results of this study suggest that sperm chromatin integrity and morphology are closely associated with each other. A disturbance in head conformation, rather than the appearance of vacuoles, is the greatest indicator of chromatin instability. However, impairment of the thermoregulatory system may cause a perturbation in cellular integrity that extends into cells that are morphologically sound. This concept is important in understanding the possible mechanisms associated with male subfertility and early embryonic mortality. This work also encourages further studies to determine the degree of additive information provided to sperm morphology by chromatin structure analysis.

REFERENCES

- Amann, RP** (1962) Reproductive capacity of dairy bulls. IV. Spermatogenesis and testicular germ cell degeneration *American Journal of Anatomy* **110** 69
- Angelopoulos T, Moshel YA, Lu L, Macanas E, Grifo JA, Krey LC** (1998) Simultaneous assessment of sperm chromatin condensation and morphology before and after separation procedures: effect on the clinical outcome after in vitro fertilization *Fertility and Sterility* **69** 740-747
- Aravindan GR, Bjordahl J, Jost LK, and Evenson DP** (1997) Susceptibility of human sperm to *in situ* DNA denaturation is strongly correlated with DNA strand breaks identified by single-cell electrophoresis *Experimental Cell Research* **10** 231-237
- Bach, O, Glander H-L, Scholz G, and Schwarz J** (1990) Electrophoretic patterns of spermatozoal nucleoproteins (NP) in fertile men infertility patients and comparison with NP of somatic cells *Andrologia* **22** 217-224
- Balhorn R** (1982) A model of the structure of chromatin in mammalian sperm *Journal of Cell Biology* **93** 298-305
- Balhorn R, Reed S and Tanphaichitr N** (1988) Aberrant protamine 1/protamine 2 ratios in sperm of infertile human males *Experientia* **44** 52-55
- Balhorn R, Corzett M, Mazrimas J, and Watkins B** (1991) Identification of bull protamine disulfides *Biochemistry* **30** 175-181
- Ballachey BE, Miller HL, Jost LK, and Evenson DP** (1986) Sperm head morphology and nuclear chromatin structure evaluated by flow cytometry in a diallel cross in mice *Canadian Journal of Genetics and Cytology* **28** 954-966
- Ballachey BE, Evenson DP, and Saacke RG** (1988) The sperm chromatin structure assay: relationship with alternate tests of semen quality and heterospermic performance in bulls *Journal of Andrology* **9** 109-115
- Barth AD and Oko, RJ** (1989) *Abnormal Morphology of Bovine Spermatozoa* Iowa State Press, Ames
- Bedford, JM, Bent, MJ, and Calvin H** (1973) Variations in the structural character and stability of the nuclear chromatin in morphologically normal human spermatozoa *Journal of Reproduction and Fertility* **33** 19-29
- Belleti, EB and Mello, MLS** (1996) Methodological variants contributing to detection of abnormal DNA-protein complexes in bull spermatozoa *Brazilian Journal of Genetics* **19** 97-103
- Bellve AR** (1972) Viability and survival of mouse embryos following paternal exposure to high temperature *Journal of Reproduction and Fertility* **30** 71-81
- Bianchi PG, Manicardi GC, Bizzaro D, Bianchi U, and Sakkas D** (1993) Effect of DNA protamination on fluorochrome staining and *in situ* nick-translation of murine and human spermatozoa *Biology of Reproduction* **49** 1038-1043
- Bianchi PG, Manicardi, GC, Bizzaro D, Campana A, Bianchi U, and Sakkas D** (1996) The use of the GC specific fluorochrome, chromomycin A3(CMA3) as an indicator of poor sperm morphology *Journal of Assisted Reproduction and Genetics* **13** 246-250
- Chowdhury AK, and Steinberger E** (1970) Early changes in the germinal epithelium of rat testes following exposure to heat *Journal of Reproduction and Fertility* **22** 205-212
- Claasens OE, Menkveld R, Franken DR** (1992) The acridine orange test: determining the relationship between sperm morphology and fertilization in vitro *Human Reproduction* **7** 242-247
- Coleman DA, Dailey RE, Leffel RE, and Baker RD** (1987) Estrous synchronization and establishment of pregnancy in bovine embryo transfer recipients *Journal of Dairy Science* **70** 858-866

- Cook RB, Coulter GH, and Kastelic JP** (1994) The testicular vascular cone, scrotal thermoregulation, and their relationship to sperm production and seminal quality in beef bulls *Theriogenology* **41** 653-671
- Coulter GH, Oko RJ, and Costerton JW** (1978) Ultrastructure of "crater" defect of bovine spermatozoa *Theriogenology* **9** 165-168
- Coulter GH** (1988) Thermography of the testes Proceedings of the 12th Technical Conference on Artificial Insemination and Reproduction 58-63
- Coulter GH and Kastelic JP** (1994) Testicular thermoregulation in the bulls *Proceedings of the 14th Technical Conference on Artificial Insemination and Reproduction* 29-34
- Courot M, and Colas G** (1986) The role of the male in embryonic mortality (cattle and sheep). In: *Embryonic Mortality in Farm Animals* pp 195-203. Ed. Sreenan JM and Diskin JM. Martinus Nijhoff, Dordrecht
- Courtens JL and Loir M** (1981) Ultrastructural detection of basic nucleoproteins: alcoholic phosphotungstic acid does not bind to arginine residues *Journal of Ultrastructural Research* **74** 322-326
- Darzynkiewicz Z, Traganos F, Sharpless T, and Melamed, MR** (1975) Thermal denaturation of DNA in situ as studied by acridine orange staining and automated cytofluorometry *Experimental Cell Research* **90** 411-428
- Degelos SD** (1995) *Separation of abnormal spermatozoa from semen produced with impaired testicular thermoregulation* Virginia Polytechnic Institute and State University (dissertation)
- DeJarnette JM, Saacke RG, Bame J, and Vogler, CJ** (1992) Accessory sperm: their importance to fertility and embryo quality, and attempts to alter their numbers in artificially inseminated cattle *Journal of Animal Science* **70** 484-491
- Dobrinski I, Hughes HPI, and Barth AD** (1994) Flow cytometric and microscopic evaluation and effect on fertility of abnormal chromatin condensation in bovine sperm nuclei *Journal of Reproduction and Fertility* **101** 531-538
- Duran EH, Gurgan T, Gunalp S, Enginsu ME, Yarali H, and Ayhan A** (1998) A logistic regression model including DNA status and morphology of spermatozoa for prediction of fertilization in vitro *Human Reproduction* **13** 1235-1239
- Dutt RH and Simpson EC** (1957) Environmental temperature and fertility of Southdown rams early in the breeding season *Journal of Animal Science* **16** 136-143
- Eid LN, Lorton SP, and Parrish JJ** (1994) Paternal influence on S-phase in the first cell cycle of the bovine embryo *Biology of Reproduction* **51** 1232-1237
- Estop AM, Munne S, Jost LK, and Evenson DP** (1993) Studies on sperm chromatin structure alterations and cytogenetic damage of mouse sperm following in vitro incubation. Studies on in vitro-incubated mouse sperm *Journal of Andrology* **14** 282-288
- Evenson DP** (1999) Loss of livestock breeding efficiency due to uncompensable sperm nuclear defects *Reproduction Fertility and Development* **11** 1-15
- Evenson DP, Darzynkiewicz Z, and Melamed MR** (1980) Comparison of human and mouse sperm chromatin heterogeneity to fertility *Science* **240** 1131-1133
- Evenson DP, Higgins PH, Grueneberg D, and Ballachey BE** (1985) Flow cytometry analysis of mouse spermatogenic function following exposure to ethylnitrosurea *Cytometry* **6** 238-253
- Evenson DP, and Karabinus DS** (1991) Early detection by flow cytometry of reduced semen quality resulting from environmental heat stress *A Research Report submitted to Select Sires, Inc.* Plain City, OH
- Evenson DP, and Jost LK** (1994) Sperm chromatin structure assay: DNA denaturability. In *'Methods in Cell Biology. Vol. 42, Flow Cytometry'*. Eds. Z Darzynkiewicz, Robinson, JP, and Crissman, HA. pp59-176 Academic Press, Inc. Orlando, FL

- Evenson DP, and Jost, LK** (2000) Sperm chromatin structure assay is useful for fertility assessment *Methods in Cell Science* **00** 1-20
- Eyestone WH, and First NL** (1989) Variation in bovine embryo development in vitro due to bulls *Theriogenology* **31** 191-196
- Fracavilla S, Cordeschi G, Gabriele A, Gianaroli L, and Properzi G** (1996) Chromatin defects in normal and malformed human ejaculated and epididymal spermatozoa: a cytochemical ultrastructural study *Journal of Reproduction and Fertility* **106** 259-268
- Fujisawa M, Hayashi A, Okada H, Arakawa S, and Kamidono S** (1997) Enzymes involved in DNA synthesis in the testes are regulated by temperature *in vitro* *European Urology* **31** 237-242
- Gledhill BL, Darzynkiewicz Z, and Ringertz NR** (1971) Changes in deoxyribonucleoprotein during spermiogenesis in the bull: increased [³H]actinomycin D binding to nuclear chromatin of morphologically abnormal spermatozoa *Journal of Reproduction and Fertility* **26** 25-38
- Gorczyca W, Traganos F, Jesionowska H, and Darzynkiewicz Z** (1993) Presence of strand breaks and increased sensitivity of DNA in situ to denaturation in abnormal human sperm cells: analogy to apoptosis in somatic cells *Experimental Cell Research* **207** 202-205
- Ibrahim ME, and Pedersen H** (1988) Acridine orange fluorescence as male fertility test *Archives of Andrology* **20** 125-129
- Johnson LA, Wilker CE, and Cerelli JS** (1994) Spermatogenesis in the bull. *Proceedings of the 15th Technical Conference on Artificial Insemination and Reproduction* 9-27
- Kapuscinski J, Darzynkiewicz Z, and Melamed MR** (1982) Luminescence of the solid complexes of acridine orange with RNA *Cytometry* **2** 201-211
- Karabinus DS, Evenson DP, Jost LK, and Baer RK** (1990) Comparison of semen quality in young and mature Holstein bulls measured by light microscopy and flow cytometry *Journal of Dairy Science* **73** 2364-2371
- Karabinus DS, Vogler CJ, Saacke RG, and Evenson DP** (1997) Chromatin structural changes in bovine sperm after scrotal insulation of Holstein bulls *Journal of Andrology* **18** 549-555
- Karnovsky MJ** (1965) A formaldehyde gluteraldehyde fixative of high osmolality for use in the electron microscopy *Journal of Cell Biology* **27** 137
- Kastelic JP, and Coulter GH** (1993) Scrotal surface, scrotal subcutaneous, intrtesticular, and intraepididymal temperatures in bulls *Proceedings of the VII World Conference on Animal Production* **3** 360-361
- Kastelic JP, Cook RB, Coulter GH, and Saacke RG** (1996) Insulating the scrotal neck affects semen quality and scrotal/testicular temperatures in the bull *Theriogenology* **45** 935-942
- Kenney RM, Evenson DP, Garcia MC, and Love CC** (1995) Relationship between sperm chromatin structure, motility, and morphology of ejaculated sperm and seasonal pregnancy In: *Biology of Reproduction Monograph Series 1, Equine Reproduction* Eds. Sharp DC, and Bazer FW Edwards Brothers, Inc.
- Kosower NS, Katayose H, and Yanagamachi R** (1992) Thiol-disulfide status and acridine orange fluorescence of mammalian sperm nuclei *Journal of Andrology* **13** 342-348
- Kraznowskia H** (1974) The passage of abnormal spermatozoa through the uterotubal junction of the mouse *Journal of Reproduction and Fertility* **38** 81-90
- Kvist U** (1982) Spermatozoal thiol-disulfide interaction: a possible event underlying physiological sperm chromatin decondensation *Acta Physica Scandanavia* **115** 503-505
- Lee LPK and Fritz IB** (1972) Studies in spermatogenesis in rats V. Increased thermolability of lysosomes from testicular germ cells and its possible relationship to impairments in spermatogenesis in cryptorchidism *Journal of Biological Chemistry* **247** 7956-7961

- Love CC and Kenney RM** (1999) Scrotal heat stress induces altered sperm chromatin structure associated with a decrease in protamine disulfide bonding in the stallion *Biology of Reproduction* **60** 615-620
- Malmgren L and Larsson K** (1989) Experimentally induced testicular alterations in boars: histological and ultrastructural findings *Journal of Veterinary Medicine* **36** 3-14
- Manicardi GC, Bianchi PG, Pantano S, Azzoni P, Bianchi U, and Sakkas D** (1995) Presence of endogenous nicks in DNA of ejaculated human spermatozoa and its relationship to Chromomycin A3 accessibility *Biology of Reproduction* **52** 864-867
- McCarthy S and Ward WS** (2000) Interaction of exogenous DNA with the nuclear matrix of live spermatozoa *Molecular Reproduction and Development* **56** 235-237
- McCosker PJ** (1969) Abnormal spermatozoan chromatin in infertile bulls *Journal of Reproduction and Fertility* **18** 363-365
- McPherson S, and Longo FJ** (1993) Chromatin structure-function during mammalian spermatogenesis: DNA nicking and repair in elongating spermatids *European Journal of Histochemistry* **37** 109-128
- Miller D, Hrudka M, Cates WF, and Mapletoft R** (1982) Infertility in a bull with a nuclear sperm defect: a case report *Theriogenology* **17** 611-621
- Mitchell JR, Senger PL, and Rosenberger JL** (1985) Distribution and retention of spermatozoa with acrosomal and nuclear abnormalities in the cow genital tract *Journal of Animal Science* **61** 956-963
- Orgebin-Crist M, and Jahad C** (1977) Delayed cleavage of rabbit ova after fertilization by young epididymal spermatozoa *Biology of Reproduction* **16** 358-363
- Pace MM, Sullivan JJ, Elliot FI, Graham EF, and Coulter GH** (1981) Effects of thawing temperature, number of spermatozoa and spermatozoal quality on fertility of bovine spermatozoa packaged in 0.5-ml French straws *Journal of Animal Science* **53** 693-701
- Pardoll DM, Vogelstein B, and Coffey DS** (1980) A fixed site of DNA replication in eukaryotic cells *Cell* **19** 527-536
- Parrish JJ, and Eid L** (1994) In vitro fertilization and its relationship to bull fertility *Proceedings of the 15th Technical Conference on Artificial Insemination and Reproduction* 68-73
- Prieto M, Maki AH, and Balhorn R** (1997) Analysis of DNA-protamine interactions by optical detection of magnetic resonance *Biochemistry* **36** 11944-11951
- Qiu J, Hales BF, and Robaire B** (1995) Effects of chronic low-dose cyclophosphamide exposure on the nuclei of rat spermatozoa *Biology of Reproduction* **52** 33-40
- Robbins RK, Saacke RG, and Chandler PT** (1976) Influence of freeze rate, thaw rate, and glycerol level on acrosomal retention and survival of bovine spermatozoa frozen in French straws *Journal of Animal Science* **42** 145-154
- Roux C, and Dadoune JP** (1989) Use of acridine orange staining on smears of human spermatozoa after heat-treatment; evaluation of the chromatin condensation *Andrologia* **21** 275-281
- Saacke RG, Bame JH, Karabinus DS, Mullins KJ, and Whitman S** (1988) transport of abnormal spermatozoa in the artificially inseminate cow based upon accessory sperm in the zona pellucida. *11th International Congress on Animal Reproduction and Artificial Insemination* Dublin, Ireland
- Saacke RG, Nadir S, Dalton J, Bame J, DeJarnette, Degelos S, and Nebel RL** (1994) Accessory sperm evaluation and bull fertility-An update *Proceedings of the 15th Technical Conference on Artificial Insemination and Reproduction* Columbia, MO
- Saacke RG, DeJarnette JM, Bame JH, Karabinus DS, and Whitman S** (1998) Can spermatozoa with abnormal heads gain access to the ovum in artificially inseminated super- and single-ovulating cattle? *Theriogenology* **51** 117-128

- Saacke RG, Dalton J, Nadir S, Nebel RL, and Bame J** (2000) Relationship of seminal traits and insemination time to fertilization rate and embryo quality *Animal Reproduction Science* **60-61** 663-667
- Sailer BL, Jost LK, and Evenson DP** (1995) Mammalian sperm DNA susceptibility to in situ denaturation associated with the presence of DNA strand breaks as measured by terminal deoxynucleotidyl transferase assay *Journal of Andrology* **16** 80-87
- Sakkas D, Manicardi G, Bianchi PG, Bizzaro D, and Bianchi U** (1995) Relationship between the presence of endogenous nicks and sperm chromatin packaging in maturing and fertilizing mouse spermatozoa *Biology of Reproduction* **52** 1140-1155
- Sakkas D, Urner F, Bianchi PG, Bizzaro D, Wagner I, Jaquenoud N, Manicardi G, and Campana A** (1996) Sperm chromatin anomalies can influence decondensation after intracytoplasmic sperm injection *Human Reproduction* **11** 837-843
- Sakkas D, Mariethoz E, Manicardi G, Bizzaro D, Bianchi PG, Bianchi U** (1999) Origin of DNA damage in ejaculated human spermatozoa *Reviews of Reproduction* **4** 31-37
- Salisbury GW and Van Demark NL** (1961) *Physiology of Reproduction and Artificial Insemination of Cattle* W.H. Freeman and Co., San Fransisco, CA
- Sambrook J, Fritsch EF, and Maniatus T** (1989) *Molecular Cloning: A laboratory manual* Vol. 2 Cold Spring Harbor Laboratory Press, New York
- Setchell BP** (1998) The Parkes Lecture: Heat and the testis *Journal of Reproduction and Fertility* **114** 179-194
- Shaffer HE and Almquist JO** (1948) Vital staining of bovine spermatozoa with an eosin-aniline blue staining mixture *Journal of Dairy Science* **31** 677
- Skinner JD and Louw GN** (1966) Heat stress and spermatogenesis in *Bos indicus* and *Bos taurus* cattle *Journal of Applied Physiology* **21** 1784
- Sreenan JM and Diskin MG** (1983) Early embryonic mortality in the cow: Its relationship with progesterone concentration *Veterinary Record* **112** 517-521
- Steif A, Winter DM, Stratling WH, and Sippel A** (1989) A nuclear DNA attachment element mediates elevated and position-independent gene activity *Nature* **341** 343-345
- Stewart TA, Bellve AR, and Leder P** (1984) Transcription and promoter usage of the *myc* gene in normal somatic and spermatogenic cells *Science* **226** 707-710
- Tejada RI, Mitchell JC, Norman, A, Marik J, and Freidman S** (1984) A test for the practical evaluation of male fertility by acridine orange (AO) fluorescence *Fertility and Sterility* **42** 87-91
- Vogler CJ, Bame JH, DeJarnette JM, McGilliard ML, and Saacke RG** (1993) Effects of elevated testicular temperature on morphology characteristics of ejaculated spermatozoa in the bovine *Theriogenology* **40** 1207-1219
- Waites GMH and Moule GR** (1961) Relation of vascular heat exchange to temperature regulation in the testis of the ram *Journal of Reproduction and Fertility* **2** 213-224
- Ward WS** (1997) Chromosome organization in mammalian sperm nuclei. In *Genetics of Human Male Infertility* pp 205-221 Eds C Barratt, C de Jonge, D Mortimer and J Parinaud. Editions EDK, Paris
- Ward WS and Coffey DS** (1991) DNA packaging and organization in mammalian spermatozoa: comparison with somatic cells *Biology of Reproduction* **37** 569-574
- Ward WS and Zalensky AO** (1996) The unique, complex organization of the transcriptionally silent sperm chromatin *Critical Reviews in Eukaryotic Gene Expression* **6** 139-147
- Wetteman RP and Desjardins C** (1979) Testicular function in boars exposed to elevated ambient temperature *Biology of Reproduction* **20** 235-241
- Young WC** (1927) The influence of high temperature on the guinea pig testis. Histological changes and effects on reproduction *Journal of Experimental Zoology* **49** 459-499

APPENDICES

Appendix A

Egg Yolk Citrate Extender

Stock Citric Acid (5% w/v):

5 g citric acid monohydrate
Deionized water up to 100 ml

Stock Sodium Citrate

Sodium Citrate dihydrate
5.6 ml stock 5% citric acid
Deionized water up to 1000 ml

Antibiotics (GTLS)

800 µl Gentamicin (100 µl/ml)
600 µl Tylosin (500 µl/ml)
600 µl Linco-spectin (300/600 µl/ml)

Fraction A non-glycerol extender 100 ml

78 ml stock sodium citrate
20 ml egg yolk
2 ml antibiotics

Fraction B glycerol extender 100 ml

65.9 ml stock sodium citrate
20 ml egg yolk
14 ml glycerol
0.1 ml antibiotics

Appendix B

Solutions for AOA Chromatin Structure Assay

A. 2.9% Sodium Citrate Buffer Solution (prepared daily):

- 1) 2.9 % Na Citrate dihydrate + 9 mM EDTA in deionized H₂O
 - a. 400 ml buffer = 11.6 g Na Citrate dihydrate + 1.344 g EDTA
 - b. adjust pH of solution with 1M citric acid monohydrate

B. 56 mM 2-Mercaptoethanol Solution (prepared daily):

- 1) 120 μ l 2-Mercaptoethanol (2-ME; 78 MW) solution
- 2) 25 ml 2.9 % Na Citrate buffer solution

C. Carnoy's Acid treatment (prepared daily):

- 1) 30 ml methanol
- 2) 10 ml glacial acetic alcohol
- 3) 5 ml 56 mM 2-ME (7 mM final concentration of 2-ME in acid)
 - a. adjust pH to 1.2 with 4 N HCL

D. Buffer to Rinse Acridine Orange Stained Slides:

- 1) 40 ml 2.9% sodium citrate buffer + 9 mM EDTA
- 2) 5 ml 56 mM 2-ME (7 mM final concentration of 2-ME in buffer)
 - a. place in 5°C cold room before rinsing

E. Acridine Orange (AO) Stain Stock Solutions:

- 1) AO stock solution
 - a. 0.1 g very high purity AO (Polysciences, Warrington, PA)
 - b. 100 ml deionized H₂O
- 2) 0.1 M Citric Acid stock solution
 - a. 4.202 g citric acid monohydrate
 - b. 200 ml deionized H₂O
- 3) 0.3 M NH₂HPO₄·7H₂O stock solution
 - a. 4.02 g Na₂HPO₄·7H₂O
 - b. 50 ml deionized H₂O

F. AO Staining Solution (prepared daily)

- 1) 20 ml 0.1 citric acid stock
- 2) 1.25 ml Na₂HPO₄·7H₂O stock
- 3) 5 ml AO stock
 - a. pH of solution = 2.5
 - b. stain solution must be kept in the dark at 5°C until use

Appendix C

Sperm Chromatin Structure Assay (SCSA) Solutions

A. TNE Buffer Solution:

- 1) 0.01 M Tris buffer
- 2) 0.15 M NaCl
- 3) 1mM EDTA
 - a. pH = 7.4

B. Acid-Detergent Solution

- 1) 0.15 M NaCl
- 2) 0.08 N HCL
- 3) 0.1% Triton-X 100
 - a. pH = 1.2

C. AO Staining Solution

- 1) 0.2 M Na₂HPO₄
- 3) 1 mM EDTA
- 4) 0.15 M NaCl
- 5) 0.1 M citric acid
- 6) 6µg AO/ml staining buffer
 - a. pH= 6.0

CURRICULUM VITAE

Nicole Acevedo

Current Address

503 Sunridge Dr. Apt. O
Blacksburg, VA 24060
(540) 951-3306
nacevedo@vt.edu

Permanent Address

3903 Locust Lane
Alexandria, VA 22310
(703) 960-1502

EDUCATION

Master of Science, Reproductive Physiology, *Expected May 2001*

Virginia Polytechnic Institute and State University (Virginia Tech), Blacksburg, VA

Thesis: Effects of elevated testicular temperature on morphology and chromatin characteristics of ejaculated spermatozoa in the bovine.

Advisor: Richard G. Saacke

Bachelor of Science, Animal and Poultry Sciences, *May 1998*

Virginia Polytechnic Institute and State University (Virginia Tech), Blacksburg, VA

PROFESSIONAL AFFILIATIONS

Sigma XI, The Scientific Research Society, *April 2000-present*

Society for the Study of Reproduction, *June 2000-present*

RESEARCH INTERESTS

- Development of assisted reproductive technologies for both human and animal species
- Mechanisms that induce spermatozoal deficiencies in sustaining early embryonic development
- Mechanisms responsible for oocyte deficiencies in sustaining embryonic development
- Development of gamete cryopreservation techniques for endangered wildlife species
-

RELATED EXPERIENCE

Research

Graduate Research Assistant/Thesis Research, Reproductive Physiology, Department of Dairy Science, Virginia Tech, Blacksburg, VA *October 1998-present*

- Designed and conducted experiments for evaluating the effects of a mild thermal insult to the bovine testis on ejaculated sperm morphology and chromatin stability
- Cryopreserved bovine semen
- Performed standard viability examinations on spermatozoa
- Quantified morphological characteristics of ejaculated spermatozoa using differential interference contrast microscopy
- Evaluated chromatin perturbations of spermatozoa using fluorescence microscopy
- Performed flow cytometric analysis of the chromatin status of spermatozoa

Research Assistant/Undergraduate Research, Reproductive Physiology, Department of Animal and Poultry Sciences, Virginia Tech, Blacksburg, VA *October 1997-April 1998*

- Collected ram semen and aided in semen cryopreservation process
- Assessed semen quality through traditional viability examinations

- Evaluated perivitelline membrane assay as an accurate indicator of cryopreserved ram sperm viability

Research Trainee, Department of Reproductive Physiology, National Zoological Park, Washington, DC *May 1997-August 1997*

- Worked under the mentorship of Head Theriogenologist
- Compiled and computerized male and female reproduction data for endangered black-footed ferrets
- Assisted in electroejaculation procedure for semen collection and in laproscopic artificial insemination procedures
- Evaluated semen characteristics before and after cryopreservation
- Participated in anesthesia study involving domestic felids

Clinical Volunteer, National Institutes of Health Animal Center, Poolesville, MD *June 1997*

- Assisted during laproscopic insemination of domestic cat/leopard cat hybrids
- Performed physical examinations on anesthetized leopard cat hybrids
- Collected and evaluated felid blood samples to determine health status
- Recorded clinical data into medical records

Surgical Assistant, Reproductive Physiology, Department of Animal and Poultry Sciences, Virginia Tech, Blacksburg, VA *Fall 1996*

- Administered hormone treatment to ewes
- Observed artificial insemination techniques
- Assisted in surgical removal of ovine embryos

Teaching

Graduate Teaching Assistant, Reproductive Physiology, Department of Dairy Science, Virginia Tech, Blacksburg, VA *September 2000-December2000; September 1999-December1999; October 1998-December1998*

- Collaborated in administration of undergraduate reproductive physiology laboratory course
- Prepared lectures for specific laboratory sessions
- Advised students during office hours
- Helped grade lecture and laboratory examinations

ABSTRACT

Acevedo N, Bame JH, Kuehn LA, Hohenboken WD, Evenson DP, and Saacke RG. "Effects of scrotal insulation on morphology and chromatin characteristics of ejaculated spermatozoa in the bovine" (in preparation)

LANGUAGE SKILLS

- Fluent in written and spoken English and Spanish
- Partially fluent in written and spoken French